DETERMINATION OF CRITICAL MICELLE CONCENTRATION OF AN AMPHIPHILIC SIDEROPHORE

by

Kenneth Scott Mousseau

A professional paper submitted in partial fulfillment
of the requirements for the degree

of

Master of Science

in

Chemical Engineering

MONTANA STATE UNIVERSITY
Bozeman, Montana

August 2009

APPROVAL

of a professional paper submitted by

Kenneth Scott Mousseau

This professional paper has been read by each member of the thesis committee and has been found to be satisfactory regarding content, English usage, format, citation, bibliographic style, and consistency, and is ready for submission to the Division of Graduate Education.

Dr. Abigail Richards

Approved for the Department of Chemical and Biological Engineering

Dr. Ron Larsen

Approved for the Division of Graduate Education

Dr. Carl A. Fox

STATEMENT OF PERMISSION TO USE

In presenting this professional paper in partial fulfillment of the requirements for a master's degree at Montana State University, I agree that the Library shall make it available to borrowers under rules of the Library.

If I have indicated my intention to copyright this thesis by including a copyright notice page, copying is allowable only for scholarly purposes, consistent with "fair use" as prescribed in the U.S. Copyright Law. Requests for permission for extended quotation from or reproduction of this thesis in whole or in parts may be granted only by the copyright holder.

Kenneth Scott Mousseau

August 2009

DEDICATION

This work is dedicated to my primary investigator, Dr. Abigail Richards for giving me the opportunity to pursue my studies at Montana State University, as well as for her patience and guidance.

I would also like to thank all the faculty and students of the Department of Chemical Engineering and the Department of Chemistry at MSU for help and advice with my course work and research.

TABLE OF CONTENTS

TABLE OF CONTENTS – CONTINUED

LIST OF TABLES

LIST OF FIGURES

ABSTRACT

The sodachelins are a group of six amphiphilic siderophores produced by a halophilic bacterium. Amphiphilic siderophores, such as the sodachelins, are important in the solubilization and sequestration of iron related to microbial metabolism and are also unique in their ability to form micelle and vesicular structures. This professional paper describes siderophore importance in iron bioavailability, siderophore chemistry and biological function and a thermodynamic analysis of forces that drive micellization and vesicle formation. A description of experiments conducted to isolate, separate and purify the sodachelins for the purpose of measuring their critical micelle concentration (CMC) follows the review of literature. Initial siderophore isolation was achieved using XAD-2 resin to generate a crude extract. This crude extract was then purified by HPLC, and the measurement of CMC of a single siderophore, sodachelin E, was performed with a tensiomat instrument. Crude separation by XAD resin was proven successful; XAD resin has a strong affinity for siderophores as shown by experiment with the siderophore desferrioxamine B (DFB) as a control. Purification of the crude siderophore extract by only one pass on the HPLC was proven insufficient to generate a single, pure siderophore. At least a second pass on the HPLC is required to remove all contaminants. The protocol developed for CMC analysis is consistent and accurate based on a sodium dodecyl sulfate (SDS) control experiment. An approximate CMC value of 140 μM for sodachelin E was obtained, however, HPLC analysis showed contamination of another sodachelin and possible other organic solutes, indicating that this value may be inaccurate.

CHAPTER 1

INTRODUCTION

Introductory Comments

Amphiphilic siderophores, such as sodachelins, are potentially important in the solubilization and sequestration of iron related to microbial metabolism. These compounds are unique in their ability to form micelle and vesicular structures, characteristics which are of importance to industrial process engineering and have potential applications in drug delivery. This study focuses on characterization of the micelle forming capacity of sodachelin E, an amphiphilic siderophore produced by *Halomonas pantelleriensis* SL28 an isolate from a highly saline and alkaline soda lake located in Grant County in central Washington, USA. This study evaluated methods of isolating Sodachelin E using XAD-2 resin and HPLC, as well as methods of determining the Critical Micelle Concentration (CMC) using surface tension measurements. This section begins with a review of pertinent literature addressing siderophore importance in iron bioavailability, siderophore chemistry and biological function, siderophore de-chelation and iron uptake, and a thermodynamic analysis of forces that drive micellization and vesicle formation.

Iron

Iron is the fourth most abundant element of the earth and is an essential nutrient for all forms of life. Over the course of evolution, iron has become a necessary and

versatile nutrient as a component of metabolic functions and enzymes such as cytochromes in electron transport, peroxidases, catalases, and nitrogenases, to name a few (Lippard and Berg, 1994). The two common oxidation states of iron, Fe(II) and Fe(III), are important for biological life but only Fe(II) is readily available at neutral pH. The solubility of Fe(III) at neutral pH is approximately 10^{-18} M, starkly contrasting the solubility of Fe(II), which is readily available up to concentrations of 100 mM at physiological pH (Neilands, 1991). Changes in the bioavailability of Fe(III) can be attributed to the introduction of O_2 in the atmosphere, a process that began billions of years ago. As O_2 was slowly introduced into the atmosphere by photosynthetic organisms, it oxidized the surface Fe(II) to Fe(III) and created highly insoluble Fe(III) (oxyhydr)oxides (Neilands, 1991). Iron(III) has thus become a scarce nutrient for biological life, primarily in oxygen rich environments. Furthermore, iron under aerobic conditions, is extremely toxic due to its involvement in harmful Fenton type reactions (Touati, 2000). Since most microbial life requires between 10^{-8} to 10^{-6} M for optimal growth and considering the scarcity of soluble iron, most microbes would have to live in a state of permanent iron deficiency unless they can scavenge, solubilize, and store otherwise insoluble iron.

Siderophores

To solubilize and scavenge otherwise insoluble iron, organisms can sequester iron in an aerobic environment through the synthesis and excretion of low molecular weight chelating molecules known as siderophores. Siderophores are commonly produced by aerobic and facultative anaerobic bacteria, and by fungi. In 1973, Lankford coined the

term “siderophore” after the Greek words for “iron carriers”. These low molecular weight chelators are typically near 600 Da in size, but have been observed as small as 200 Da and as large as 2000 Da (Budzikiewicz, 2003; Budzikiewicz, 2005; Scott, 2003). Siderophores have a very high and specific affinity for Fe(III) with a binding constant $K_{sp} = 10^{30.0}$ or greater (Neilands, 1995). While most siderophores are water-soluble and are excreted outside the cell into the environment, there are some that are not excreted at all. An example is the mycobactins, synthesized by mycobacteria, which are located within the cell envelope (De Voss et al., 1999; Ratledge and Dover, 2000). It is common for microorganisms that do not produce siderophores to rely on siderophores from neighboring microorganisms to scavenge iron as it permits cooperation within the microbial community for the purpose of scavenging for iron. Furthermore, the ability to utilize the siderophores of the other neighboring bacteria prevents any inhibition of growth due to the complexation of iron by an unrecognizable ligand (Andrews et al., 2003).

While the production of siderophores to scavenge iron is biologically necessary for survival, there are some strains of bacteria that have evolved to live in highly iron-restricted environments, such as the *Lactobacilli*. The *Lactobacilli* only contain a few atoms of iron per cell (Archibald, 1983) and are able to thrive within dairy products containing high levels of lactoferrin and glycoprotein which tightly complex iron. These organisms need to tolerate high H_2O_2 environments and acidic environments, in which bacteria containing a great deal of iron would experience harmful Fenton-type reactions. For this reason, *Lactobacilli* utilize the vitamin B_{12}, which is a cobalt-containing

reductase for the generation of deoxynucleotide precursors for DNA synthesis (Archibald, 1983).

Biological Function of Siderophores

While a siderophore's main function is to acquire ferric iron from insoluble hydroxides or iron bound to surfaces. They can also complex iron from other both soluble and insoluble iron compounds, such as ferric citrate, ferric phosphate, Fe-transferrin, ferritin (iron bound to sugars), plant flavone pigments, glycosides, and even artificial chelators, such as EDTA (Winklemann, 2002). Although iron is biologically necessary, it is also toxic in excessive quantities due to its involvement in harmful Fenton type reactions (Touati, 2000). Free iron is thus tightly regulated in mammalian hosts through binding to proteins such as hemoglobin, transferrin, lactoferrin and ferritin. The strict homeostasis of iron leads to a very low free concentration of about 10^{-24} M in mammals (Raymond et al., 2003). Often, the survival of an invading bacterial species within a mammalian host rests on its ability to secrete siderophores that will compete with the iron-binding proteins of the host organism. For example, certain pathological bacteria such as *Bacillus anthracis* produce siderophores, bacillibacatin and petrobactin, for the purpose of sequestering iron from the host. Bacillibacatin has been shown to successfully out compete the immune system protein siderocalin and strip it of iron (Abergel et al., 2006).

Structure of Siderophores

The majority of siderophores may be divided into three main structural classes, based on the presence of hydroxamate, catecholate, and citric acid based functional

groups, as shown in Figure 1.1. Hydroxamate siderophores include examples such as ferrioxamines, ferrichromes and coprogens. Siderophores containing catecholate iron-coordinating groups include the enterobactins, vibriobactins and yersiniabactin, while carboxylate and mixed ligand α-hydroxamates include pyoverdines, azotobactins and ferribactins (Neilands, 1995). The selectivity of siderophores for iron depends upon the number and type of metal binding groups in addition to their subsequent steriochemical arrangement. To date, there are almost 500 compounds identified as siderophores that incorporate hydroxamate, catecholate and/or α-hydroxamate binding subunits arranged in various architectures, including linear, tripodal, endocyclic and exocyclic structures. These compounds comprise the most efficient iron-binding ligands found in nature (Neilands, 1995).

The number of iron-binding groups, or denticity, is an important component of the siderophore structure. Bidentate and tetradentate siderophores have been identified and show affinity for iron, but hexadentate siderophores appear to be the most common due to their ability to bind to all six of Fe(III)'s coordination sites (Boukhalfa and Crumbliss, 2002). Hexadentate siderophores are based on hydroxamate and/or catecholate binding subunits and have a very high affinity for Fe(III) and a lower affinity for Fe(II) (Granger and Price 1999). This is observed when comparing two hexadentate siderophores desferrioxamine B (DFB) and desferrioxamine E (DFE). When DFB and DFE bind to Fe(III), a stability constant of $10^{30.6}$ and $10^{32.5}$ can be observed, respectively, but the stability constants observed when bound with Fe(II) are $10^{10.0}$ and $10^{12.1}$, respectively (Spasojovec et al., 1999).

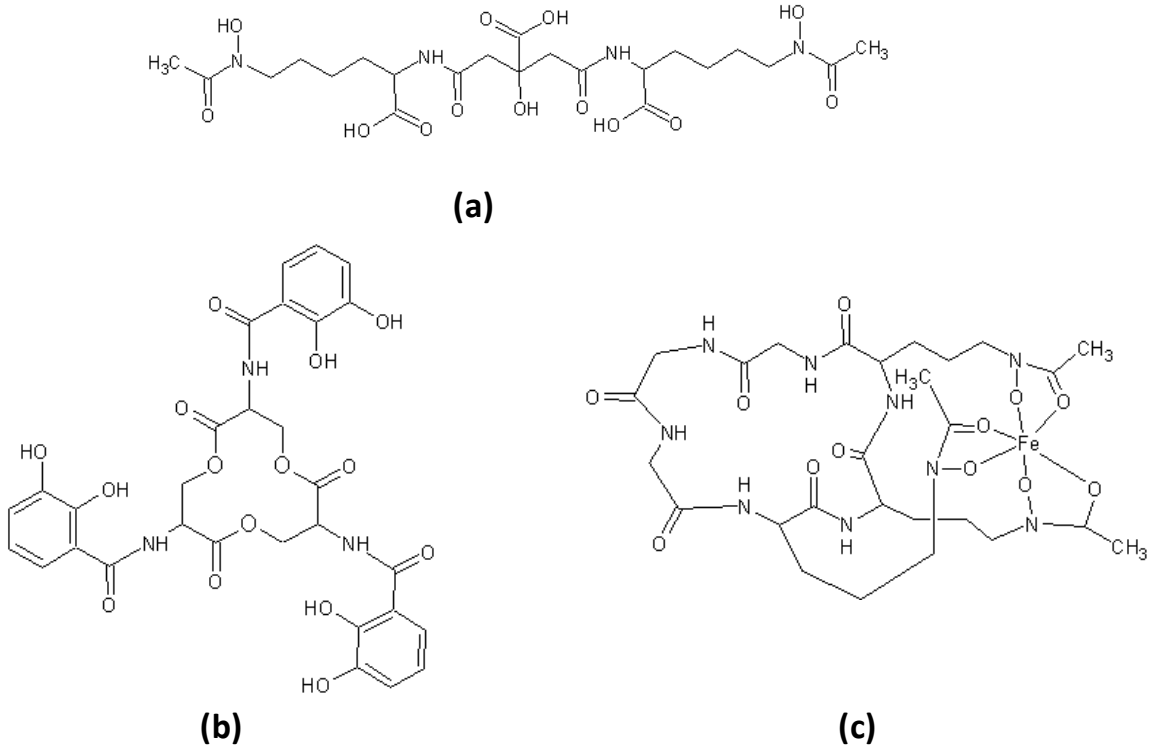

Figure 1.1. Siderophores representing hydroxamate, catecholate and α-hydroxycarboxylic acid based structures: (a) aerobactin, (b) enterobactin and (c) ferrichrome.

The slight difference in stability constants for DFB and DFE can be attributed to enhanced binding affinity of the siderophore. DFB is a linear siderophore while DFE is a macrocyclic siderophore. Cyclization enhances complex stability, thus improving resistance to degrading enzymes. Cyclization is regarded as a common feature of secondary metabolism and is found in microbial peptides, polyketides, macrocyclic antibiotics and other bioactive compounds (Winklemann, 2002).

<u>De-Chelation of Bound Iron</u>

Once Fe(III) has been bound by siderophores outside the cell, the iron must be delivered to the cell and released from the siderophore complex. The overall scheme of

siderophore-mediated iron uptake is reasonably well defined (Winkelmann, 1991; Winklemann and Carrano, 1997; Sigel and Sigel, 1998). The high stability of iron-siderophore complexes makes ligand dissociation thermodynamically unfavorable and slow inside the cell. One proposed method is proton-catalyzed de-chelation, although the rate of complete dissociation from the ligand is slow under acidic pH conditions (Boukhalfa et al., 2000). Partial de-chelation of a hexadentate chelate at one bidentate subunit is fast, partial de-chelation of the subunit increases the number of free coordination sites on the iron center, thus decreasing the affinity of the Fe(III) binding with the siderophore. Fe(II)-siderophore complexes are 20 orders of magnitude less stable that their Fe(III) counter parts, as stated previously, and when sites on the iron become available, the siderophores loses some of its affinity for iron. Protonation of a hexadentate Fe(III)-siderophore complex and reduction of the Fe(III)-siderophore complex, followed by a competitive ligand exchange, seems to be the most viable mechanism for iron release under physiological conditions (Boukhalfa and Crumbliss, 2002). The redox potential of most siderophore-bound Fe(III) complexes are in the range of -350 mV to -750 mV, which places them out of the range of most biological reducing agents such as NADPH or NADH (E = -320 mV) (Boukhalfa and Crumbliss, 2002). The redox potential of stable iron complexes shifts to more positive values upon reduction of Fe(III) to Fe(II) and thus falls within the range of biological reducing agents such as NADPH.

Iron-Siderophore Cell Uptake

As mentioned previously, microbes produce siderophores to accumulate appropriate levels of iron. Iron-siderophore complexes are typically too big to diffuse into cells through the cell wall or through porins. The paradigm of siderophore-mediated uptake of Fe(III), for terrestrial bacteria, is that bacteria make and then secrete siderophores into the surrounding environment. The siderophores then solubilize and coordinate Fe(III), at which point the Fe(III)-siderophore complex is recognized by a siderophore-specific cell surface receptor that actively transports the Fe(III)-siderophore complex into the bacterium. The biosynthesis of these receptors, which are a type of gated protein channel, is co-regulated with siderophore biosynthesis in response to low iron levels (Guerinot, 1994). The uptake of Fe(III) through this mechanism is certainly energy dependent and once transported, the Fe(III)-siderophore complex is shuttled from the periplasm to the cytoplasm by a permease within the cytoplasmic membrane (Koster, 1991; Mietzner et al., 1998; Boos, 1996).

Current Siderophore Research

While hundreds of siderophores have been identified, most are produced by terrestrial or disease-causing microorganisms. The study of siderophores produced in marine environments is relatively new and has identified several novel and prominent structural features (Butler, 2005). One unique class of marine siderophores is found to facilitate the reduction of Fe(III) when exposed to UV light (Barbeau et al., 2001). Another class, some of which also induce the photoreduction of Fe(III), are amphiphilic and contain unique peptidic head-groups appended by one of a series of fatty acid tails

(Martinez et al., 2000; Martinez et al., 2003). An amphiphilic molecule is a molecule that contains a hydrophilic head-group with a hydrophobic appendage, such as a phospholipid.

Of the amphiphilic peptidic siderophores identified to date, the fatty acid chain is appended at the amine terminus of the peptidic head-group and varies in length from C_{10} to C_{18}. The amphiphilic peptidic siderophores are strikingly similar compounds, consisting of an Orn-Ser-Orn carboxyl motif in which each Orn is hyrdroxylated and acetylated to from the hydroxamic acid moiety that coordinates Fe(III). An example of this can be seen in Figure 1.2 (Martinez et al., 2000; Martinez et al., 2003; Xu et al., 2002). Some are excreted extracellularly such as the aquachelins and the marinobactins (Martinez et al., 2000), while others, such as the amphibactins, contain longer C_{18} fatty acid tails and remain cell associated. The amphiphilic siderophore-producing marine microorganisms typically generate a suite of siderophores unique for each organism. A *Marinobacter* species produces six amphiphilic siderophores known as marinobactin A, B, C, D_1, D_2 and E (Figure 1.2). Each of these siderophores differs only by fatty acid chain length or level of saturation and maintains a conserved peptidic head-group. Similarly, there are four known aquachelins A, B, C and D, that vary only in chain type produced by *Halomonas aquamarina* (Martinez et al., 2000). Like other amphiphilic compounds found in nature, amphiphilic siderophores have the ability to form micelles and vesicles.

Not all amphiphilic siderophores found in nature are restricted to marine environments. The ornibactins are amphiphilic siderophores that were isolated from the

terrestrial bacterium *Burkholderia cepacia*, but these siderophores contain much shorter fatty acid appendages that range in length from C_4 to C_8 (Stephen et al., 1993; Meyer et al., 1995).

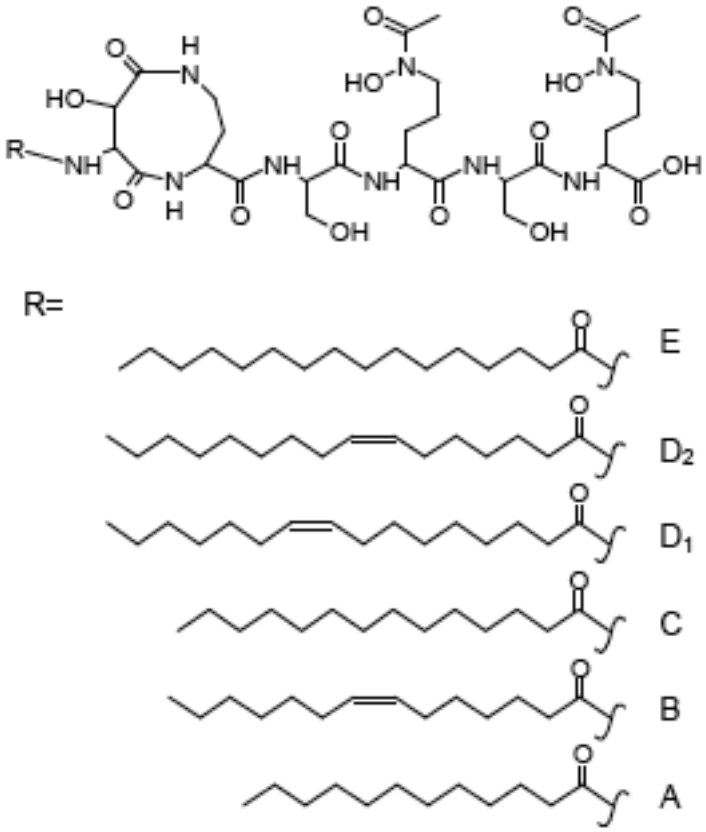

Figure 1.2. Marinobactin A-E: amphiphilic siderophore isolated from a marine environment.

Although many of the marine siderophores are amphiphilic, some siderophore producing marine bacteria produce siderophores that lack a fatty acid tail altogether. One example is *Alteromonas luteoviolacea*, which produces two structurally similar siderophores known as alterobactin A and B (Reid et al., 1993).

Solutions of amphiphilic compounds tend to aggregate into spherical colloids upon reaching a critical concentration. This critical concentration is known as the critical micelle concentration (CMC). A micelle in aqueous solutions forms a spherical-like aggregate with the hydrophilic head regions along the outer surface in contact with a surrounding polar solvent, sequestering the hydrophobic tail portion in the center of the aggregate. Many of the marine siderophores, because of their amphiphilic nature, are predisposed to behave in such a manner and aggregate as micelles. Thermodynamic properties, to be explained later in this chapter, are the sole driving force behind the formation of amphiphilic compounds into micelles.

Surface Tension

Surface tension is a physical property of liquid that depends on intermolecular forces. It is described as a skin-like barrier observed at the liquid-gas interface. Surface tension has dimensions of force per unit length or energy per unit area; both are equivalent by dimensional analysis. In other words, surface tension is the amount of energy required to increase the surface area of a liquid.

To better explain the concept of surface tension, imagine a container filled with water and open to the atmosphere to create a liquid-gas interface. In the bulk of the liquid, each molecule is pulled equally in all directions by surrounding liquid, resulting in no net force. At the interface, liquid experiences an attractive force inward by the molecules in the bulk of the liquid and little to none, by comparison, to the molecules in the gas phase at the interface. Thus, molecules at the interface experience a net inward force towards the bulk of the solution that is only balanced by the liquid's resistance to

compression (Figure 1.3). However, there is a thermodynamic driving force present to diminish the amount of surface area of the liquid resulting in a "skin-like" barrier.

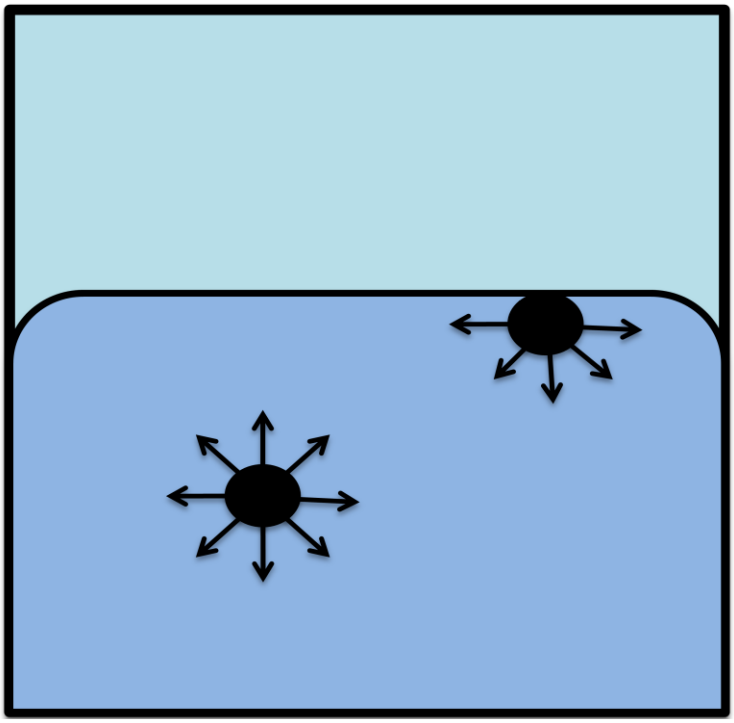

Figure 1.3. Diagram of forces on two molecules of liquid. In the bulk of the liquid, the molecules are pulled equally in all directions, resulting in no net force. At the surface, the molecules are pulled inward by other molecules toward the bulk of the liquid.

Dissolved substances, depending on their structure, can affect the surface tension of a liquid. Inorganic salts can increase the surface tension of a liquid while alcohols decrease surface tension with increasing concentration. Surfactants (or amphiphiles) also decrease surface tension with increasing surfactant concentration until a minimum is reached, after which little to no further effect is observed. Surface tension is also dependent on temperature. The general trend is that surface tension decreases with

increasing temperature until the critical temperature of the fluid is reached, at which point the surface tension is zero (Hiemenz, 1986).

Thermodynamics of Surface Tension

Thermodynamics requires that all spontaneous changes of state be accompanied by a decrease in Gibbs free energy (G). As mentioned previously, surface tension is the amount of mechanical work needed to increase the surface area of a liquid.

$$\text{Work} = F\,dx = \gamma\,dA \qquad (1)$$

Equation (1) relates work to surface tension, where F represents force, x is length, γ represents the surface tension of a liquid in units of energy per unit area and A will be the surface area of the film with units of length squared. Thermodynamic work is a path dependent process, as mobile surfaces have a tendency to decrease spontaneously in area, a decrease in area corresponds to work done by the system and an increase in area requires work to be done on the system; equation (1) is then negative. The first law of thermodynamics states that the energy of the system equals

$$dE = \delta q - \delta w \qquad (2)$$

in which δw is the work done by the system and δq is the heat absorbed by the system. The work term, δw, can be divided into the pressure-volume (P,V) term and the non-pressure-volume components. The second law tells us that, in order for a process to be reversible, the heat (δq) in equation (1) becomes $\delta q_{rev} = T\,dS$ where T represents temperature and S is entropy. With these stipulations imposed, equation (2) can be rewritten as,

$$dE_{rev} = T\,dS - pdV - \delta w_{non\text{-}pV} \qquad (3)$$

Equation (3) can thus be substituted into the fundamental definition of Gibbs free energy, yielding equation (4).

$$dG_{rev} = T\,dS - p\,dV - \delta w_{non\text{-}pV} + p\,dV + V\,dp - T\,dS - S\,dT \quad (4)$$

This is a fundamental equation of physical chemistry, which illustrates the physical significance of Gibbs free energy. Equation (4) shows that for a constant pressure and constant temperature in a reversible process that Gibbs free energy equals the maximum work associated with a reversible process.

$$dG = -\delta w_{non\text{-}pV} \quad (5)$$

Subbing the relationship of non-pV work from Equation (1) into Equation (5), a relationship between Gibbs energy per unit increment of area is observed.

$$dG = \gamma\,dA \quad (6)$$

$$\gamma = \left(\frac{\partial G}{\partial A}\right)_{T,p} \quad (7)$$

Equation (7) illustrates why decreasing the surface area of a mass of liquid is always a spontaneous process provided it is not coupled to any other energy changes. G^S is another notation that is often encountered, which emphasizes the fact that γ is identical to the excess Gibbs free energy per unit area arising from the surface. In this way, the energy interpretation of γ has been identified with a specific thermodynamic function. Many of the general relationships that apply for Gibbs free energy equations also apply equally to surface tension. For example, one of the most familiar definitions of Gibbs free energy is the fundamental equation $G = H - TS$, where H is the enthalpy, S is the entropy, and T is for temperature. The fundamental equation for Gibbs energy for surface

tension can be written as Equation (8) where H^s is the enthalpy per unit area and S^s the entropy per unit area.

$$G^s = \gamma = H^s - TS^s \qquad (8)$$

Differentiating Equation (8) with respect to temperature yields the following relationship for entropy.

$$\left(\frac{\partial G^s}{\partial T}\right)_p = \left(\frac{\partial \gamma}{\partial T}\right)_p = -S^s \quad (9)$$

Equation (9) shows the influence of surface tension and temperature on the entropy of a liquid surface. The surface entropy can provide a very useful description of the molecular interactions in the interface of the liquid (Birdi, 1997). Therefore, by default, the surface enthalpy depends on both the surface tension and its derivative with temperature at a constant pressure.

$$H^s = \gamma - T\left(\frac{\partial \gamma}{\partial T}\right)_p \qquad (10)$$

The enthalpy of surface tension is assumed to be nearly temperature independent due to the fact that as γ decreases with temperature and the product of the surface tension derivative (with temperature) increases as temperature increases (Hiemenz, 1986). Equation (10) shows that an amount of heat must be generated and absorbed by the liquid when the surface is extended. The reason that heat is absorbed upon extending a surface is that the molecules must be transferred from the interior against the inward attractive force to form the new surface.

Thermodynamics of Micelle Formation

In nature, there is a continuous transition between true solutions, colloidal solutions, and organized systems such as liquid crystals. Solutions of amphiphilic compounds are particularly interesting because of their capacity to self-assemble in solution into micelles. In the simplest surfactants, equilibrium exists between monomers and micelles. However, such micelles will change in size and shape depending on the conditions: temperature, pressure, concentration and the presence of electrolytes. Further, depending on the chain length, the chemical structure and geometry of the surfactant molecules, and the presence of other solutes, these systems can adopt a vast number of structures (Owen et al., 2007; Luo et al., 2002a; Sommerdijk et al., 1999; Desnoyers and Perron, 1997).

For simplicity, it is sufficient to consider a binary system of a very dilute non-ionic solute in water. In this example, there are basically two kinds of interactions: solute-solvent and solute-solute. For aqueous micellar systems, the polar head group of the surfactant always remains in contact with water. The principal solute-solvent interaction involved in the micellization process is, therefore, hydrophobic hydration, although modification of the hydrophilic hydration of the head group will result from head-group interactions in the palisade layer of the micelle. Hydrophobic hydration is the driving force that forces non-polar molecules to form aggregates in water. Pure water molecules adopt a structure that maximizes entropy. A hydrophobic molecule will disrupt this structure and decrease entropy to create a cavity that is unable to interact with water. To counter this decrease in entropy, water molecules push hydrophobic molecules

together to decrease the surface area of the hydrophobic molecules and this maximizes the entropy.

The most common method of determining Gibbs free energy of micellization is the pseudo-phase model for non-ionic solutes.

$$\Delta G^M = RT \ln CMC \qquad (11)$$

The ΔG^M represents the Gibbs free energy for micellization, CMC is the critical micelle concentration, R is the gas law constant and T is temperature. When mole fractions are used in Equation (11), ΔG^M directly measures the free energy difference per mole between surfactant molecules in micelles and in water. The thermodynamic criterion for phase equilibrium is that the chemical potential of the surfactant must be the same in the micelle and in water. Micellization is a spontaneous process initiated when a particular surfactant reaches a particular concentration. The Gibbs-Helmholtz equation provides another thermodynamic relationship that defines the contributions of Gibbs free energy in micellization.

$$\Delta H^M = \left(\frac{\partial \left(\Delta G^M / T \right)}{\partial \left(1/T \right)} \right)_p = -RT^2 \left(\frac{\partial \ln CMC}{\partial T} \right)_p \qquad (12)$$

The enthalpy of micellization is thus positive for non-ionic surfactants and negative for ionic surfactants. This result is most likely due to ionic interactions such as long-range coulombic interactions, similar to the ones that occur amongst electrolytes, which have a greater impact on enthalpy than any other thermodynamic terms (Israelachvili et al., 1977). The standard thermodynamic quantity for entropy can be seen below in Equation (13).

$$\Delta S^M = -\left(\frac{\partial \Delta G^M}{\partial T}\right)_p \qquad (13)$$

For micellization of non-ionic solutes, entropy values are positive and make large contributions to the Gibbs free energy. It may seem surprising that the entropic contribution is positive; after all, the number of independent kinetic units is decreasing. The key to understanding this entropy increase is the extensive hydrogen bonding that occurs in water and the hydrophobic effect. Other thermodynamic quantities such as heat capacity are not significantly affected upon micellization. Typically, heat capacities are sensitive to changes in hydrophobic interactions rather than electrostatic ones (Desnoyers and Perron, 1997; Nagarajan and Ruckenstein, 1991).

The CMC represents a fundamental micellar quantity describing the self-aggregation of amphiphilic molecules in solution. The CMC is defined as the concentration of surfactants above which micelles are spontaneously formed. Surfactants generally partition at the interface in aqueous solutions and reduce the system free energy by limiting the contact of hydrophobic portions with water. Upon reaching the CMC that is unique for all surfactants, the surfactants begin aggregating into micelles and further decrease the system's free energy.

The CMC is a physical property can be ascertained in several ways. One very popular method is measuring surface tension. As mentioned previously, the addition of surfactants to water lowers the surface free energy, thus lowering the energy required to increase the surface area of the liquid. Until CMC is reached, the surface tension of water decreases and at the CMC, little to no further change to the surface tension of water occurs. Surface tension is by no means the only property of the solution to show

discontinuity when plotted against increasing concentration of surfactants. Properties such as conductivity, turbidity, and osmotic pressure also show abrupt changes at the point at which CMC is achieved. Typically after the CMC is surpassed, the concentration of micelles increases in a linear fashion (Hiemenz, 1986).

Micelle Formation by Amphiphilic Siderophores

Several aquatic bacteria such as *Halomonas aquamarina, Marinobacter, Vibrio* and *Ochrobactrum* all produce a siderophore with a unique head group that coordinates Fe(III) and one of a series of fatty acid tails (Martinez and Butler, 2007). A particular marine bacteria known as *Marinobacter* has been studied extensively by Butler et al. (Martinez et al., 2000; Owen et al., 2007). This *Marinobacter* species, as mentioned previously, produces six known amphiphilic peptidic siderophores known as the marinobactins. These are comprised of a conserved polar head-group consisting of an Orn-Ser-Orn carboxyl motif and one of a series of appended fatty acid tails (Martinez et al., 2000). Like most surfactants found in nature or produced industrially, they have the ability to form micelles and reduce the surface tension of water. The iron-free marinobactins have very low and unique CMC values depending on their alkyl chain lengths. The shorter chain marinobactins have a CMC of 150 μM where as the CMC for the longest chain marinobactin is around 25 μM (Martinez and Butler, 2007; Martinez et al., 2000; Owen et al., 2007). This relationship is consistent with known trends of CMC values, which decrease with increasing fatty acid tail length, for surfactants such as sodium dodecyl sulfate versus sodium decyl sulfate (Szymcyck and Janczuk, 2009). The

marinobactins will most likely follow the same trends thermodynamically upon micellization. However, the marinobactins are Zwitterionic and most likely will have a larger enthalpy term compared to their non-ionic solutes due to the coulombic interactions with the polar head-groups. Upon ferration, the marinobactins still behave as a surfactant but the CMC for each agent is slightly lower (Martinez et al., 2000).

An interesting trait of the marinobactin micelles is the decrease in their diameter upon coordination of Fe(III). The diameter of an iron-free marinobactin micelle is typically 4.0 nm and the diameter of the same micelles with each siderophore constituent coordinating iron is 2.8 nm (Owen et al., 2005). The decrease in micellar diameter upon Fe(III) addition is likely due to a change in molecular geometry of the head-group upon iron coordination. The ratio of the head-group area-to-tail volume for the largest of the marinobactin siderophores likely increases upon coordination of Fe(III), giving it a more conical geometry (Israelachvili et al., 1980).

Micelle to Vesicle Transition

Marinobactins not only form micelles, in fact, they can also form unilamellar multilamellar vesicles. A vesicle, like a micelle, is a sometimes spherical colloid composed of surfactants arranged to decrease surface contact area of hydrophobic components in water. Vesicles tend to be multi-layered, like that of a cell membrane, with the hydrophobic portions of the surfactant interacting with one another and the hydrophilic components in contact with water. The process of vesicle formation appears to be spontaneous for marinobactins with the addition of excess Fe(III). Little is known about the exact thermodynamic properties involved in metal-induced vesicle formation of

single tailed micelles. However, it is safe to assume that the thermodynamic forces that drive micelles formation are similar to those involved in vesicle development (Israelachvili, 1980).

Initially at the CMC for marinobactin siderophores, micelles up to 4.6 nm in diameter form. With the addition of one equivalence of Fe(III), the marinobactin micelle shrinks to a size of approximately 3.5 nm in diameter. When a small excess of Fe(III) is added to the medium, spherical unilamellar vesicles are formed that are approximately 100-200 nm in diameter (Martinez et al., 2000; Herrington et al., 1993). With the addition of a greater excess of Fe(III) or ferrated micelles, the unilamellar vesicles begin to form multi-lamellar vesicles up to 200 nm in diameter, and in some instances, stacked bi-layers. An example of a unilamellar vesicle can be seen in Figure 1.4 (Owen et al., 2005; Owen et al., 2008; Xu et al., 2002; Beck et al., 2002).

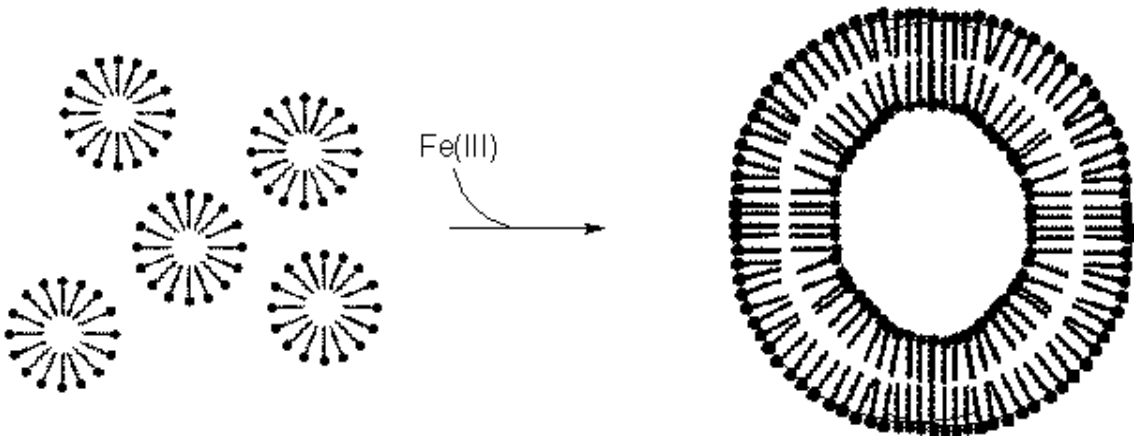

Figure 1.4. A representation of the phase change from micellar assembly of the amphiphilic siderophores to vesicle formation upon the addition of iron. Figure not drawn to scale.

Amphiphilic siderophores, like the marinobactins, are single-chained surfactants with a polar head-group. Single-chain surfactants typically only form micelles and not multi-lamellar vesicles because of their large polar head-groups and relatively small non-polar tails which promote conical-shaped molecules (Israelachvili et al., 1980). Generally, only the doubly tailed amphiphiles tend to form vesicles. Surfactants with multiple alkyl tails have a more rod-like geometry that favors a vesicular arrangement, whereas cone-shaped monocephalic surfactant molecules are thermodynamically predisposed to forming micelles (Israelachvili et al., 1980).

Research has shown that vesicle formation of single-chained surfactants with large head-groups is possible upon the addition of metal cations. Micelle to vesicle transition can result from the coordination of a transition metal ion to multiple surfactant head-groups (Owen et al., 2005; Luo et al., 2002a; Luo et al., 2002b). Bridging of the head-groups of multiple surfactants by the metal ion (Figure 1.5) effectively produces a composite surfactant molecule with two or more alkyl tails (Luo et al., 2002a; Luo et al., 2002b; Sommerdijk et al., 1999). In the case of marinobactin, it is hypothesized that excess Fe(III) induces vesicle assemblies by bridging the terminal carboxyl moieties of two or three ferrated-marinobactin siderophores. This effect is not unique for Fe(III), as it has also been reported that other metals such as Zn(II), Cd(II), La(II), etc., are also capable of binding to marinobactin siderophores and inducing vesicular aggregation (Owen et al., 2007; Luo et al., 2002a).

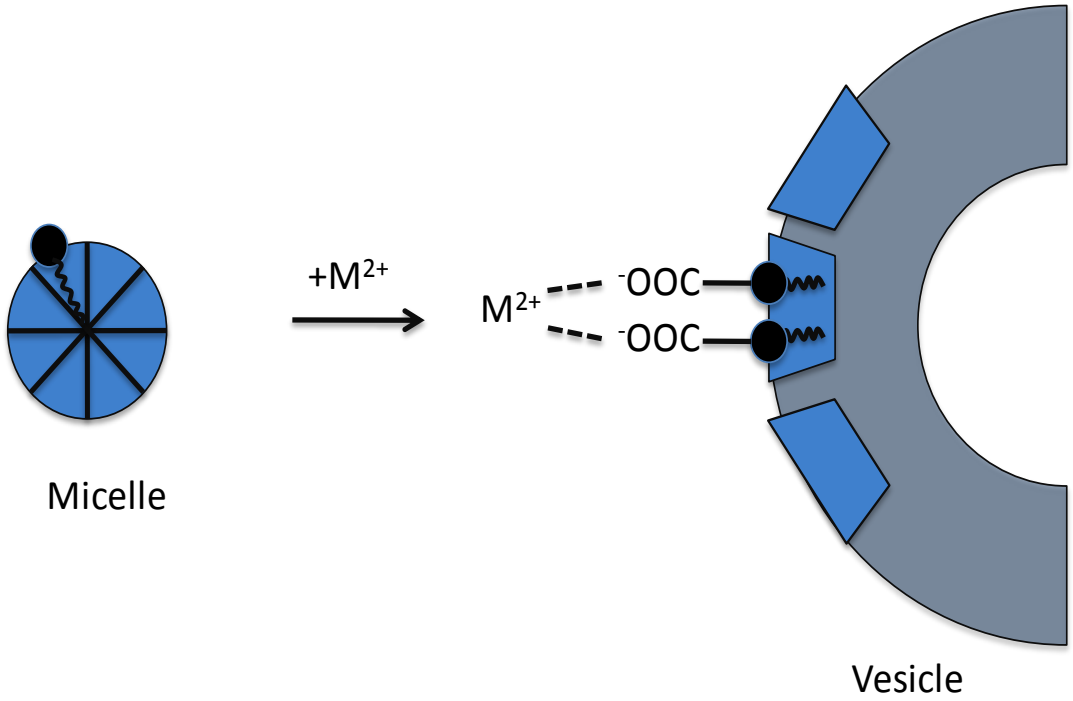

Figure 1.5. Proposed cation-induced carboxylate cross linking of ferrated siderophore head-groups to promote micelle to vesicle transition. The bridging of the head groups by a metal could pull them closer together resulting in lowering the head group area : tail volume ratio, that favors vesicle formation.

Vesicles and micelles are of great importance in pharmacologic design. Delivery of labile peptide drugs and vaccines to desired biological sites is problematic because of hydrolytic degradation, poor oral adsorption, fast clearance, and poor permeation into cells. The encapsulation of drugs and vaccines into liposomes (a.k.a. vesicles) is of great interest. This approach can be very useful to protect the peptide against first-pass metabolism, to facilitate absorption, and to slow clearance of hydrophilic peptides only if the lapidated derivatives can be subsequently converted into the parent peptides through an enzymatic reaction at the site of delivery. Lipopeptides tightly packed into vesicle-like structures would be protease resistant (Lee et al., 1999). Since proteases and other

degradative enzymes are widely dispersed in ocean water, the micelle to vesicle transition could prove to be a desired physiological advantage to increase concentration in the aggregate or increase the residence time of siderophores in such a habitat (Lee et al., 1999).

Soap Lake and Soap Lake Bacteria

Little is known about the methods used by halophilic and alkalphilic organisms to acquire iron in environments where it is scarce. *Halomonas* species are ubiquitous in saline and alkaline environments (Jones et al., 1998; Ventosa et al., 1998) and some *Halomonas* species, such as *Halomonas aquamarina*, are known to produce a suite of siderophores (Martinez et al., 2000). Soap lake was the focus of a recent study where siderophore production by the inhabitants was investigated. This study identified several siderophore producing isolates with some of the siderophores resembling amphiphilic siderophores found in the marine environment.

Soap Lake is a soda lake located in Grant County in central Washington State, USA within the Grand Coulee Basin. Soda lakes are environments that contain high concentrations of sodium carbonate and sodium bicarbonate relative to other soluble salts and thus represent a very specific type of saline lake. These environments have selected for a consortium of obligately alkalphilic and often halophilic microorganisms, because of the stable conditions of alkaline pH and frequently elevated dissolved solids concentration. Soap Lake, like many soda lakes, is alkaline with an average pH of 9.9 that is observed throughout the column of water. The lake has no inlet or outlet streams and the only source of nutrients and water comes from runoff and precipitation (Sorokin

et al., 2007; Anderson, 1958). A unique feature of Soap Lake is that it is meromictic, as it possesses two distinct layers that do not intermix. The upper layer of the lake, termed the mixolimnion layer, is brackish, containing approximately 15 g/L dissolved solid and is aerobic. The lower layer of the lake contains a much higher dissolved solids concentration, reaching 140 g/L, is much colder (6 to 8 ^{o}C) and anaerobic (Sorokin et al., 2007).

Soap Lake is home to many bacteria (Richards, 2007; Dimitriu et al., 2005; Sorokin et al., 2007). One specific bacterium of the genus *Halomonas*, most closely related to *Halomonas pantelleriensis,* designated *Halomonas pantelleriensis* SL28, is found to produce a suite of six amphiphilic siderophores (sodachelins A-F) that have been structurally characterized (Richards, 2007). Like other siderophores produced by bacteria in marine environments, the sodachelins are amphiphilic. They have a common iron coordinating peptidic head group consisting of seven amino acids linked to a fatty acid carbon chains that range from 10 to 14 carbons (Figure 1.6). The iron-coordinating groups include two hydroxylated and acetylated ornithine residues and one β-hydroxyaspartate residue. When exposed to UV light, these siderophores facilitate a photolytic reduction of Fe(III) to Fe(II) along with the cleavage of the siderophore located at the β-hydroxyaspartate residue. Because the sodachelins are similar in structure to the marinobactins, Richards hypothesized that the sodachelins will form micelles and possibly vesicles upon the addition of iron (Richards, 2007). The work to be described later tests that hypothesis.

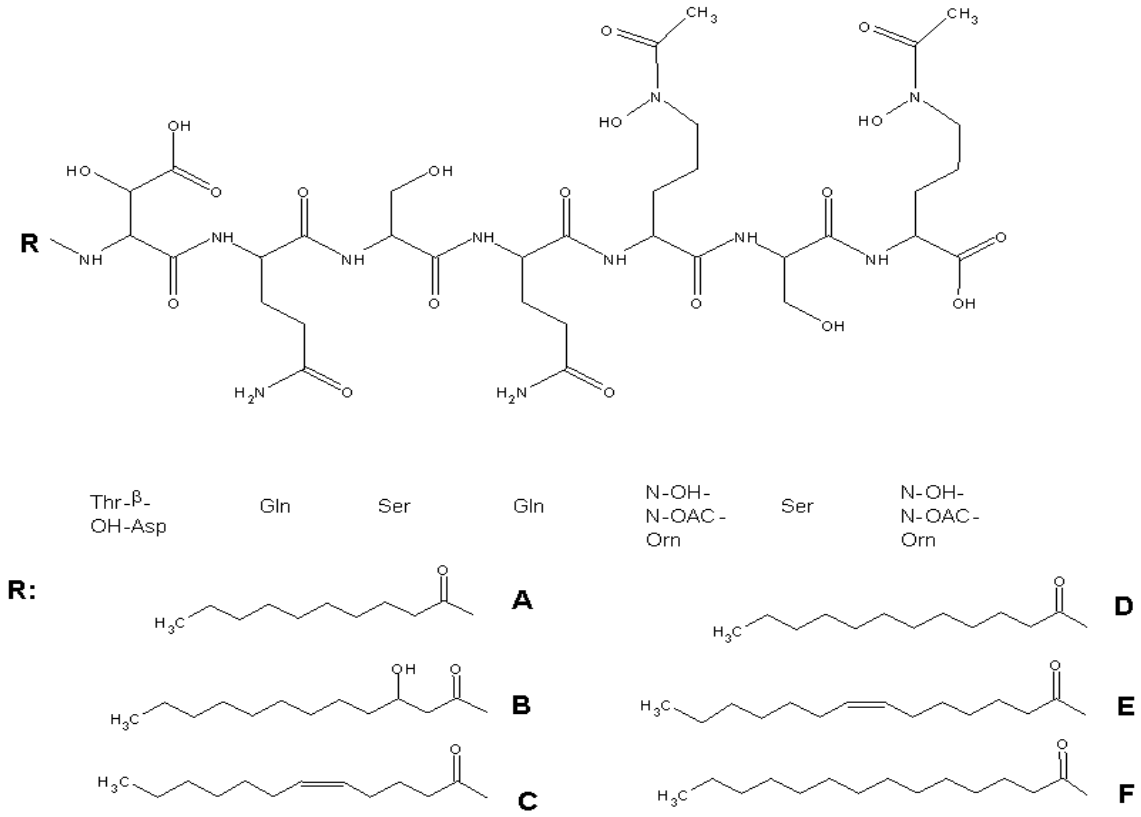

Figure 1.6. Sodachelins A-F: amphiphilic siderophores from Soap Lake isolate SL28.

Concluding Remarks

Metal-chelating surfactants are attracting much attention, particularly in the self-assembly process (Luo et al., 2002a; Luo et al., 2002b; Martinez et al., 2000; Sommerdijk et al., 1999). Richards (2007) and Butler et al. (2005) have reported suites of amphiphilic siderophores similar in structure produced by marine bacteria of different environments. Owen et al. (2005) have shown interesting aggregation behavior in the marinobactin, a suite of siderophores produced by *Marinobacter* sp. DS40M6 to facilitate the acquisition of iron (Martinez et al., 2000). The structural similarities of the sodachelins could

possibly exhibit the same aggregation behavior as the marinobactins. Understanding the mechanism by which amphiphiles undergo a micelle-to-vesicle transition is of great importance from a physiological and microbial point of view. This study attempts to characterize the CMC of sodachelin E, one of six amphiphilic siderophores produced by *Halomonas pantelleriensis* SL28, develop an operating protocol for the use of a tensiometer in measuring surface tension and test the protocol against an alternative surfactant, sodium dodecyl sulfate (SDS).

CHAPTER 2

METHODS

Experimental Goals

Iron is one of the earth's most abundant crustal elements, however Fe(III) is in short supply due to the formation of highly insoluble ferric hydroxides formed (10^{-18} M at neutral pH) in aerobic environments. To overcome scarcity of iron under iron-limited conditions, many aerobic microorganisms produce and secrete iron chelating components known as siderophores, which are low molecular weight molecules with a high specificity for ferric iron. A wide range of structures has been determined for siderophores produced by terrestrial and enteric bacteria (Winkelmann, 1991; Albrecht-Gary and Crumbliss, 1998). Several suites of marine siderophores, marinobactins and aquachelins, possesses surfactant properties and form micelles at low concentrations (Martinez et al., 2000). The sodachelin siderophores, described in Chapter 1, are similar in structure to the marinobactins and aquachelins and may also form micelles. The potential to form micelles was explored through a series of surface tension experiments. In order to perform these experiments, milligram quantities of the sodachelin siderophores must be produced, isolated and purified. This chapter describes the techniques used to produce, characterize and purify these siderophores as well as the experimental procedures used to determine their ability to form micelles. In brief, *Halomonas pantelleriensis* SL28 was grown in a high salt medium at a pH of 9.0 for approximately three days, at which time, the suite of siderophores secreted by SL28 were

crudely isolated by XAD-2 resin and furthered purified by HPLC/UV. Of the six siderophores secreted by SL28, sodachelin E, was furthered analyzed for its amphiphilic properties (CMC) in nanopure water at a neutral pH using a Tensiomat instrument.

Materials and Methods

Growth Medium

Isolate SL28 was shaken aerobically at 140 rpm and 37^{o}C in acid-washed 1 L baffled shaker flasks which contained the following components in an iron-limited medium that was adapted from Dimitriu et al. (2005) (g/L); NaCl, 50; $Na_2B_40_7$, 1.12; NH_4Cl, 1.0; $CaCl_2 \cdot 2H_2O$, 0.06; $MgCl_2 \cdot 6H_2O$, 0.05; $NaNO_3$, 0.85; KH_2PO_4, 0.50; KCl, 0.01; deferrated yeast extract, 0.25; sodium pyruvate, 5.0. The pH of the medium was adjusted to 9.0 with a 6N NaOH. This iron-limited medium stimulated siderophore production by enhancing iron-stress seen by the cells and maximized siderophore production observed in the supernatant. All components used in the Soap Lake Media were purchased from Fisher with the following exceptions: $Na_2B_40_7$, KCl and Yeast Extract. $Na_2B_40_7$ was purchased from Polarchem, KCl from Sigma and Yeast Extract from Difco. The medium was then filter sterilized using a Corning Filter System with a pore size of 0.22 μm.

Iron Removal from Complex Media Components.

Iron was removed from the yeast extract component of the SL28 growth medium using a Chelex-100 resin that was purchased from Sigma Chemical. A concentrated solution of yeast extract (50 g/L) was made and the resin was prepared according to

manufacturer's instruction. In brief, the resin was washed with five bed volumes of nanopure water followed by two bed volumes of 1 M HCl, then another five bed volumes of nanopure water and two bed volumes of 1 M NaOH and finally washed with additional five bed volumes of nanopure water. The resin was added in a 10:1 ratio (mass of complex media to mass of resin) and stirred for 45 minutes. The resin was then removed by filtration and the concentrated yeast extract was transferred to an acid washed container (Domingue et al., 1990).

Siderophore Detection by Chrome Azurol S

Siderophores were detected and quantified using the chrome azurol S (CAS) liquid method with the siderophore desferrioxamine B (DFB, Sigma-Aldrich) as the positive control (Schwyn and Neilands, 1987). The following method produces a 250 mL of CAS assay solution. A series of solutions were made with the following components and concentrations: 10 mM, hexadecyltrimethylammonium bromide (HDTMA, Sigma) in nanopure water; 1 mM $FeCl_3 \cdot 6H_2O$ (Fisher) in 10 mM HCl; 2 mM CAS (Fisher); 1 M 5-sulfosalicyclic acid (Sigma) in nanopure water. Six mL of HDTMA solution was added to a 100 mL volumetric flask and diluted with nanopure water followed by 1.5 mL of iron solution and 7.5 mL of CAS solution. While the previous solution was stirring slowly, 4.307 g of anhydrous piperazine (Acros) was placed into a separate flask with water and 6.25 mL of 12 M HCl is added. The two solutions were combined in a 100 mL volumetric flask and brought to volume with nanopure water.

For siderophore detection, a 1 mL sample of the supernatant was removed and centrifuged to remove the cells. A 20 μL volume of 5-sulfosalicyclic acid solution was

added to a cuvette followed by 0.5 mL of supernatant from centrifugation and 0.5 mL of CAS assay solution. The mixture in the cuvette reacted for 1 to 6 hours before absorbance was measured. During experiments where siderophore and optical densities were measured with respect to time, liquid samples were removed at regular intervals and measured at 630 nm for the CAS assay and 600 nm for optical density to monitor cell growth.

Qualitative Chemical Analyses for Iron-Binding Functional Groups

The siderophores were tested for the presence of hydroxamate moieties through the Csáky assay with DFB as the control (Csáky, 1948). The assay detects the presence of secondary hydroxamates and depends on the oxidation to nitrite and the formation of a colored complex via diazonium coupling. A series of solutions were made for the assay, including (g/L): sulfanilic acid (Sigma) in 30% glacial acetic acid, 10; I_2 (Aldrich) in glacial acetic acid, 13; $NaAsO_2$ (Sigma) in water, 20; sodium acetate (Fisher) in water, 350; α-napthylamine (Sigma) in 30% acetic acid. A 1 mL sample of siderophore/supernatant sample was combined with 1 mL of 6N H_2SO_4 and autoclaved for 30 minutes followed by the sequential addition of 3 mL of sodium acetate solution, 1 mL of sulfanilic acid solution and 0.5 mL of iodine solution. The mixture was allowed to incubate for 5 minutes at room temperature followed by sequential addition of 1 mL of sodium arsenite solution, 1 mL of α-napthylamine solution and diluted with water to a volume of 10 mL. The solution incubated for 20-30 minutes and was observed for color change. The clear solution will turn pink in the presence of hydroxamate moieties, and the magnitude of the change was measured by absorbance at 526 nm.

The colorimetric Arnow assay was used to detect the presence of catecholate groups in culture supernatants, with 2,3-dihydroxybenzoate (Sigma) used as a positive control (Arnow, 1937). To 1 mL of supernatant/siderophore solution the following were added sequentially: 1 mL of 0.5 N HCl, 1 mL nitrite-molybdate solution, and 1 mL of 1 N NaOH. The nitrite-molybdate solution consisted of 10 g of sodium nitrite (Fisher) and 10 g of sodium molybdate (Fisher) dissolved in 100 mL of water. The Arnow assay solution should turn from yellow to red in the presence of catecholates. The magnitude of the change was measured by absorbance at 510 nm.

Siderophore Isolation.

To test the affinity of the Amberlite XAD-2 resin (Supelco), a control experiment of 100 µM of DFB solution was made in soap lake media followed by addition of 75 g of XAD resin. The slurry was allowed to stir for one hour taking samples every six minutes and DFB concentrations being measured by CAS assay.

Deferrated high cell growth medium was inoculated with a 24 hr culture of *Halomonas* sp. strain SL28. After approximately 44 hours of incubation the presence of siderophores was confirmed using the CAS liquid assay. The culture medium was centrifuged (6000 g, 20 min, 4^{o}C, Sorvall floor model rotor). The supernatant was decanted from the cell pellet and the cell pellet was discarded. The siderophores were isolated from the high-salt medium using XAD-2 resin. Some 75 g of dry resin was added to one liter of supernatant and shaken at 140 rpm for one hour to adsorb organic compounds. The supernatant-XAD slurry was poured into 5.0 x 40 cm column and washed with one column volume of nanopure water followed by one bed volume of

100% methanol. Upon completion, the XAD resin was washed with two column volumes of nanopure water. The SL28 siderophores were eluted from the column using 100% methanol. The fractions that contained the siderophores were collected and concentrated by rotary evaporation. The concentrated samples were then filtered again to remove any solids.

As a control for the XAD resin isolation procedure, the cell-free supernatant was passed through Bond Elut solid phase extraction C_2 cartridges (Varian Inc.), which were conditioned by five bed volumes of methanol followed by five bed volumes of nanopure water. The media supernatant was passed through the C_2 cartridge and assayed for siderophore activity using the CAS liquid assay. Supernatant still retaining siderophore activity was passed through the cartridge again, the saturated solid phase was then washed with three bed volumes of nanopure water and eluted with three bed volumes of 100% methanol. The crude siderophore extract was then concentrated in a rotary evaporator.

The concentrated crude siderophore extract underwent further purification on a Vydac C-4 column (25 X 1 cm) using a Dionex ICS-3000 high performance liquid chromatography (HPLC) system. The mobile phase consisted of water/acetonitrile with 0.01% trifluoroacetic acid (TFA) (A = 99.99% Water/0.01% TFA; B = 80% acetonitrile/19.99% water/0.01%TFA). TFA is used as an ion pairing agent. Siderophores were eluted using a gradient 0% B to 60% B for 40 minutes followed by 60% B to 80% B for 10 minutes, then 80% B for 5 minutes followed by 0% B for 5 minutes more. The flow rate was maintained at 1 ml/min and the elution compounds

were monitored at an absorbance of 220 nm using a Dionex AD20 absorbance detector. Siderophores eluted into six fractions with the first beginning around 39 minutes and the last at 51 minutes. Peaks were collected by hand. Iron binding fractions were then concentrated by centrifugal evaporator and lyophilized.

Critical Micelle Concentration

A control experiment was performed with SDS (Sigma) to determine the accuracy of the Surface Tensiomat Model 21 instrument purchased from Fisher. The platinum iridium ring used by this instrument has an average circumference of 6.0001 cm and the temperature of the solution was recorded with each measurement. A series of dilutions was made from a stock solution of SDS ranging from 0.1 mM to 50 mM. The dilutions were then placed in 20 mL acid washed glass petri dishes and the ring was washed with nanopure water, then again with methanol and flamed to remove any possible contaminants. The platform that supports the vessels containing the SDS solution was adjusted for optimal measurement height to allow the ring to penetrate the surface of the solution to a depth of approximately 1/8 inch and fixed in place to maximize consistency. The instant the platinum iridium broke the surface of the solution in question was noted as time zero. The surface was allowed to settle for thirty seconds prior to initiating the semi-automatic mode of the tensiometer to increase accuracy.

A purified sample of sodachelin E (Figure 2.1) was collected by HPLC, located at 47 minutes on the HPLC chromatogram, then lyophilized to a yellowish crystalline dry product and re-suspended in nanopure water. A series of dilutions was then made generating concentrations ranging from 1 µM to 385 µM. The critical micelle

concentration was measured by using the Surface Tensiomat Model 21 instrument. The analysis and preparation of sodachelin E measurements were made in the same manner as the SDS experiment described above.

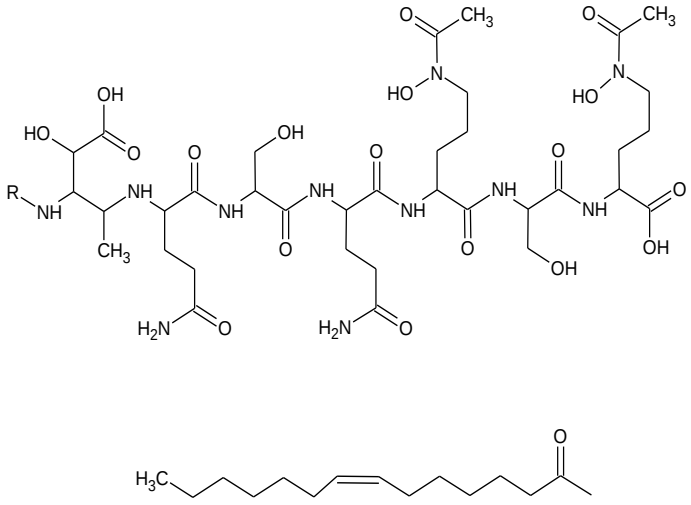

Figure 2.1. Sodachelin E from Soap Lake Isolate SL28.

CHAPTER 3

RESULTS

SL28 Growth, Siderophore Production and Identification

SL28, one of thirty isolates from Soap Lake, is of the genus *Halomonas* and produced a significant amount of siderophore (~25 µM DFB equivalence in the case of Figure 3.1) when grown on an iron-limited liquid medium in acid washed glassware. Figure 3.1 shows siderophore production reached a maximum at 44 hours of growth in mid-stationary phase. The Csàky and Arnow assays were used to determine the presence of hydroxamate and catecholate moieties. As expected, based on the chemical structure of the sodachelins (Richards, 2007), the siderophores isolated from SL28 were found to contain hydroxamate functionality by the Csàky assay while catecholates were not detected by the Arnow assay.

Siderophore Isolation

Sodachelin siderophores were successfully isolated for experimental use from SL28. To test the affinity of the XAD resin for siderophores using DFB as a model siderophore compound, a 1 L solution of 120 µM was prepared and 75 g of XAD resin was added and allowed to stir vigorously for an hour while taking samples approximately every five minutes. Tests of the resin's affinity show little to no DFB present in the solvent after 60 minutes. This indicated, for DFB, that the XAD resin has a strong affinity for DFB and thus siderophores, which can be seen in Figure 3.2.

Free ions and salts were removed using an XAD separation and further analyzed by HPLC/UV. Figure 3.3 is an HPLC/UV chromatogram that shows the elution of six peaks over a time interval of approximately 38-51 minutes, which indicated the production of a suite of six compounds (Figure 1.6). Fractions defined by these peaks were collected, each of which showed siderophore activity by the CAS assay. The retention time of these siderophores was from 38 to 51 minutes (Table 3.1) which reconfirms that the suite of siderophores produced were of large molecular weight and contained non-polar characteristics.

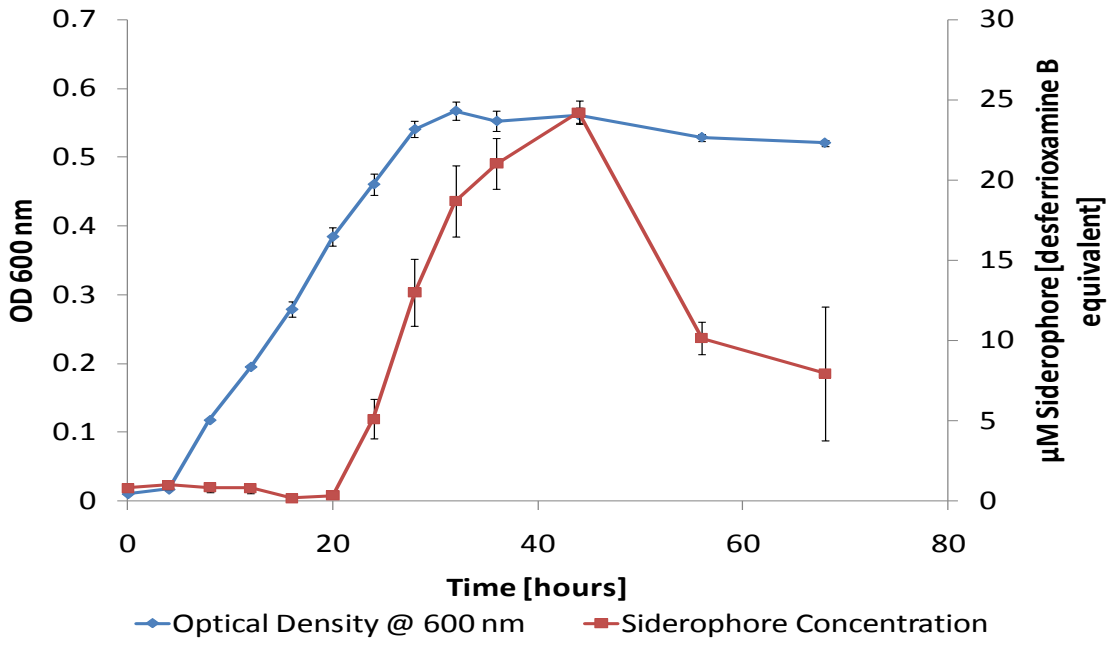

Figure 3.1. Siderophore production by Halomonas sp. strain SL28 with respect to time. Data points are averages of three replicate experiments and error bars represent the standard deviation.

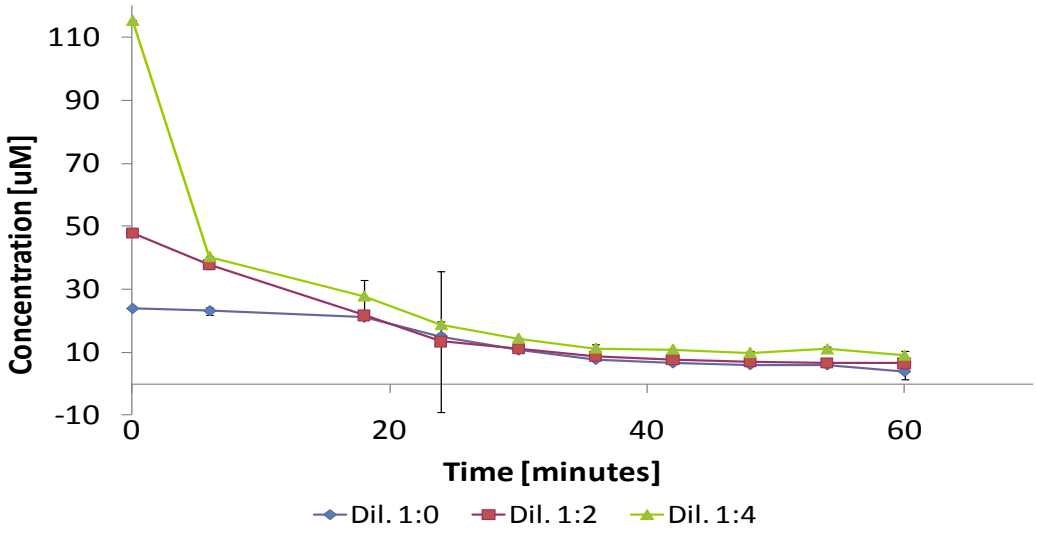

Figure 3.2. Absorption of DFB in 5 g/L Soap Lake Media On XAD Resin. Samples were diluted to ensure measurements were made within the optimum detection range of the instrument.

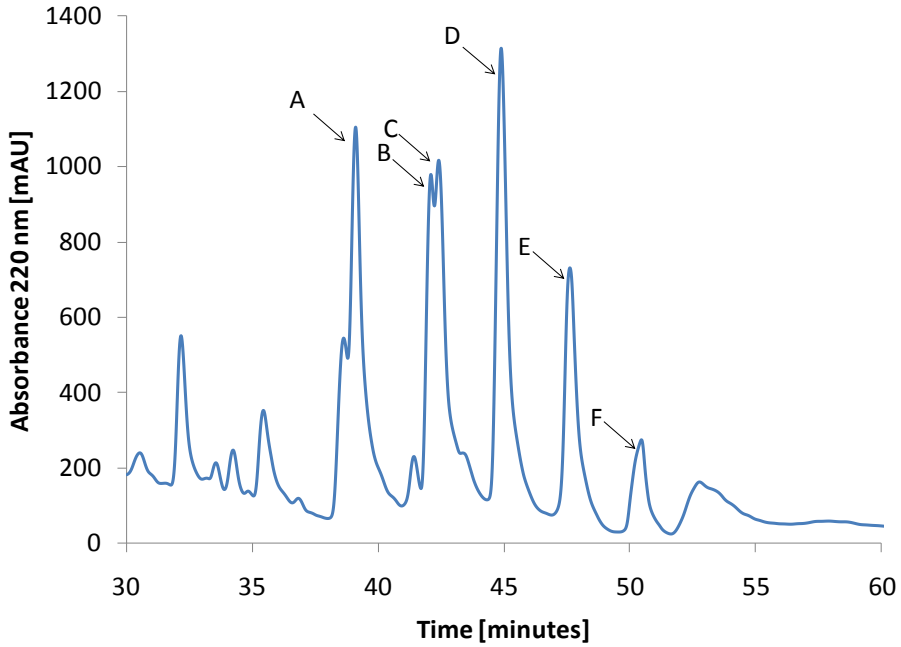

Figure 3.3. HPLC/UV chromatogram of sodachelin siderophores eluted from a C4 column. The peak labels correspond to the suite of six sodachelins from Soap Lake isolate SL28. Refer to Figure 1.6 for their structures.

Table 3.1. HPLC/UV retention times for the suite of sodachelins produced by SL28 on a Vydac C-4 column.

Siderophore	Retention Time [minutes]
sodachelin A	38.72
sodachelin B	41.72
sodachelin C	42.17
sodachelin D	44.72
sodachelin E	47.42
sodachelin F	50.45

CMC Determination

The CMC for sodachelin E was determined using the Tensiomat. The Tensiomat is a very time sensitive instrument to use in the sense that the amount of time allowed to pass after submersion of the ring, and the rate at which tension is applied to the torsion arm directly influence measurement accuracy. Submergence of the ring constitutes a significant disturbance of the surface, so the time allowed between submersion and breakaway of the ring is of great importance for consistency. The amount of time allowed for the surface to reach an equilibrium state after the ring was submerged in this experiment was 30 seconds. The data in the following graph (Figure 3.4) show the results of a timed experiment that was performed with concentrations of SDS (CMC = 8.2 mM) below the CMC (5 mM) and at a concentration above the CMC (10 mM). This particular experiment was performed to determine the optimal amount of time needed for the surface of the liquid to settle after being disturbed by the ring breaking the surface. In

Figure 3.4, one of the surface tension measurements were made using the full manual mode (5 mM manual mode), with tension applied by hand from the user, in an attempt to keep the total time spent on the measurement process around 30 seconds, from the first moment of tension applied to the point of the ring breaking free from the surface. The full manual mode was not nearly as consistent as the semi-auto mode, wherein tension was applied to the ring at a constant rate by the instrument's electric motor while the user adjusted the platform that holds the vessel by hand. The data from the semi-auto mode was far more consistent than the data from the manual mode therefore all subsequent experiments were done in the semi-auto mode.

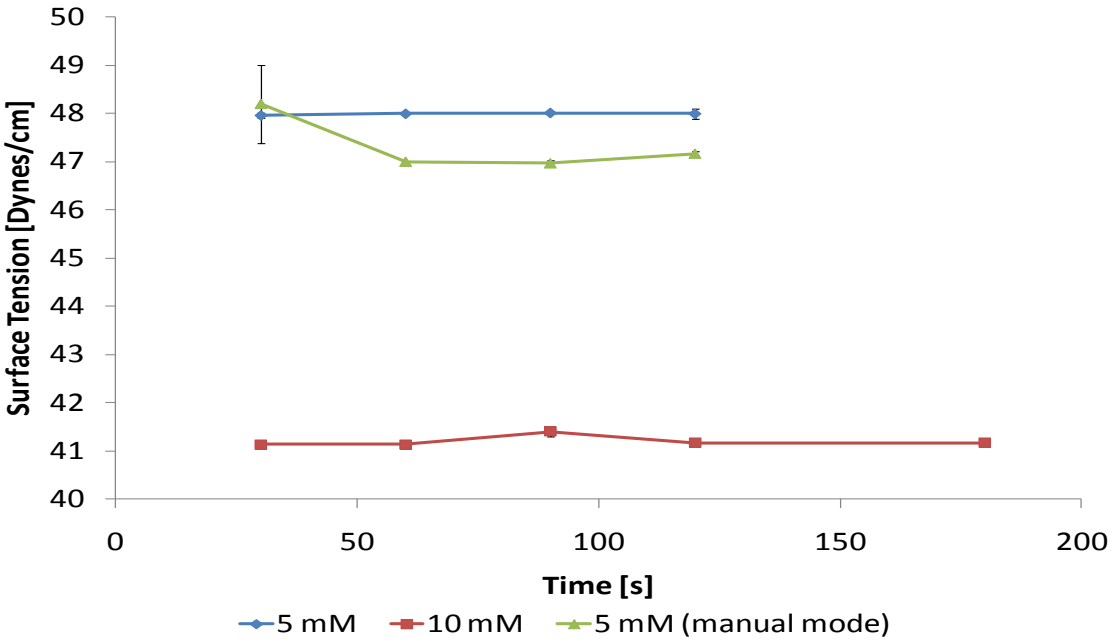

Figure 3.4. Surface settling time experiment with SDS in semi-auto mode versus full manual mode. Semi-auto mode curves are flat with very little error.

A trial experiment was performed, with the aid of SDS, to determine the accuracy of the instrument for ascertaining the CMC values for amphiphiles. The results shown in Figure 3.5 depict an inflection point in the curve between 8 mM and 9 mM, which is consistent with published data confirming the CMC of SDS of 8.2 mM.

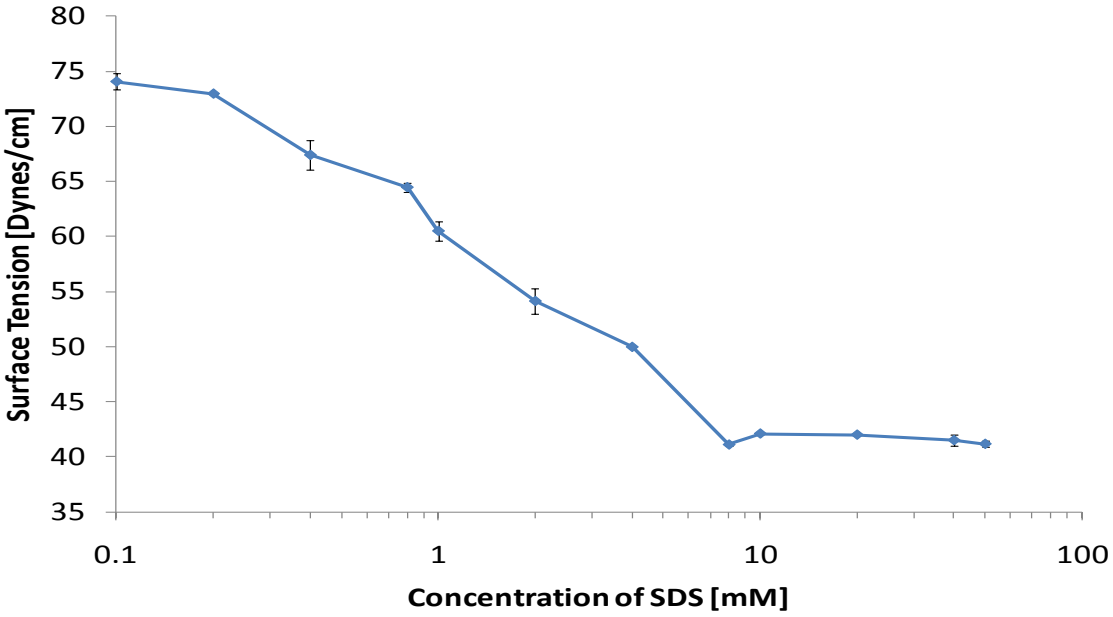

Figure 3.5. Control CMC experiment with SDS. Point of inflection is around 8-9 mM, which is consistent with published data (SDS CMC = 8.2 mM).

The first attempt at ascertaining a CMC value for sodachelin E, as shown in Figure 3.6, appears to be inconclusive potentially due to an insufficient amount of sodachelin E in the solution to promote micellization. The insufficient amount is most likely due to the presence of impurities, based on HPLC/UV analyses of the sodachelin E stock solution, as shown in Figure 3.7. It is also possible that the predicted concentration range to obtain a CMC value was incorrect. However, due to time constraints, the sample was re-concentrated and a series of more concentrated solutions were made.

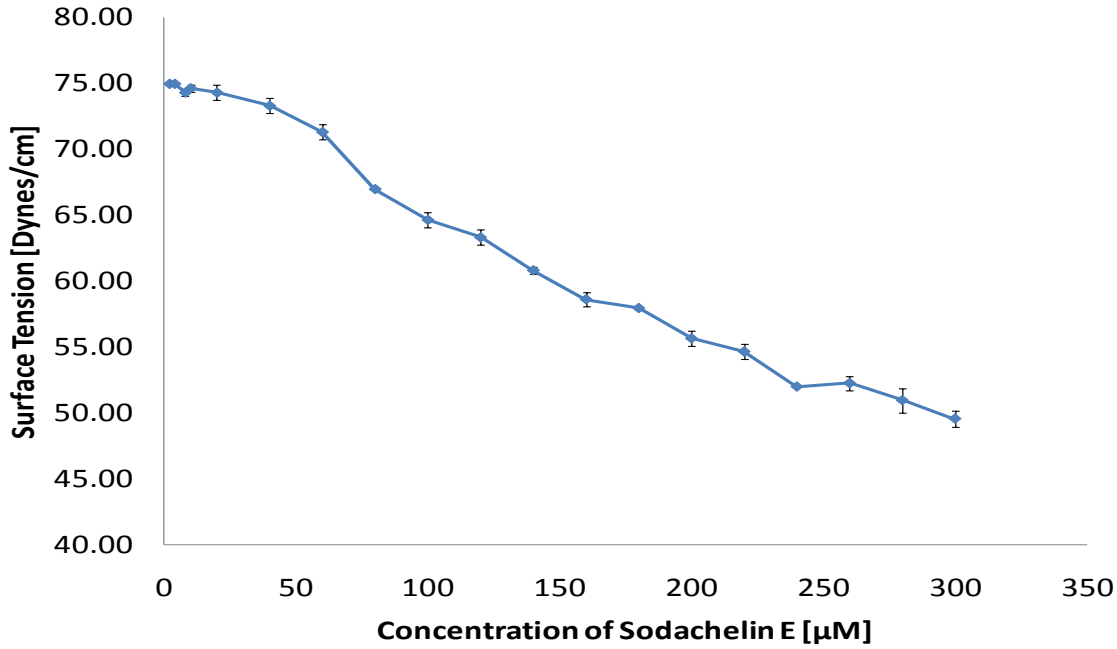

Figure 3.6. Experimental data from the first attempt of obtaining a CMC value for sodachelin E. Insufficient amount of sodachelin E present to promote micellization.

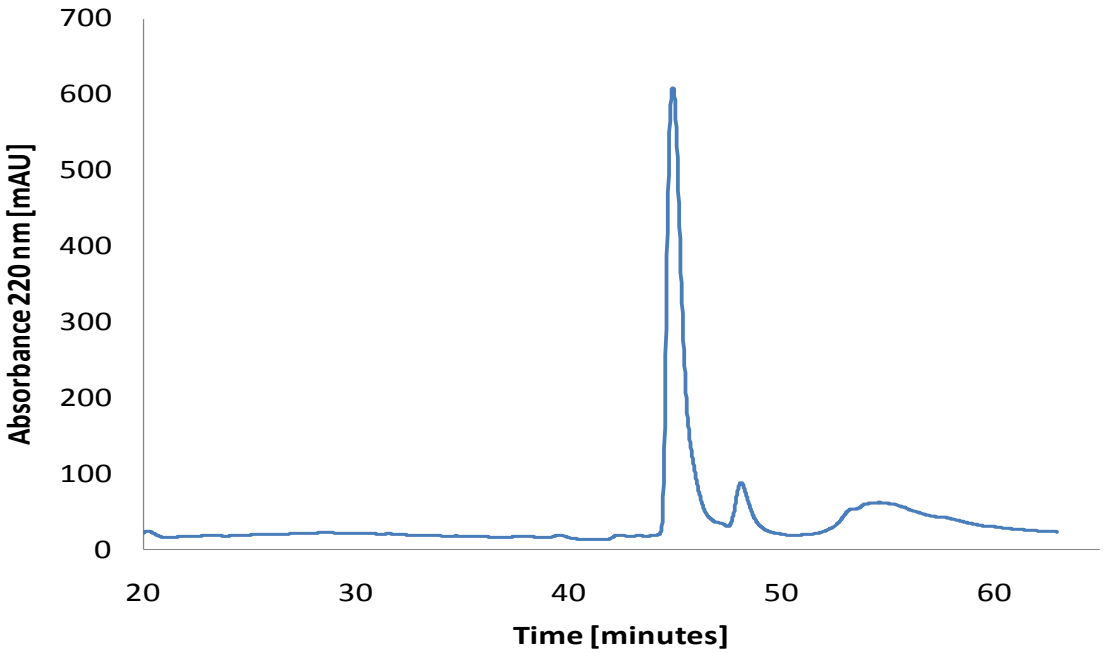

Figure 3.7. HPLC/UV chromatogram of sodachelin E stock solution used for CMC experiments. A small amount of sodachelin F is present as well as some other unknown organic contaminant.

The results of the second experiment to determine the CMC for sodachelin E can be seen in Figure 3.8. According to the graph, a point of inflection occurred between 140 µM to 150 µM. One of the dilutions was tested further by HPLC/UV and the results were exactly the same as in Figure 3.7. Therefore, the exact value of the CMC is still undetermined.

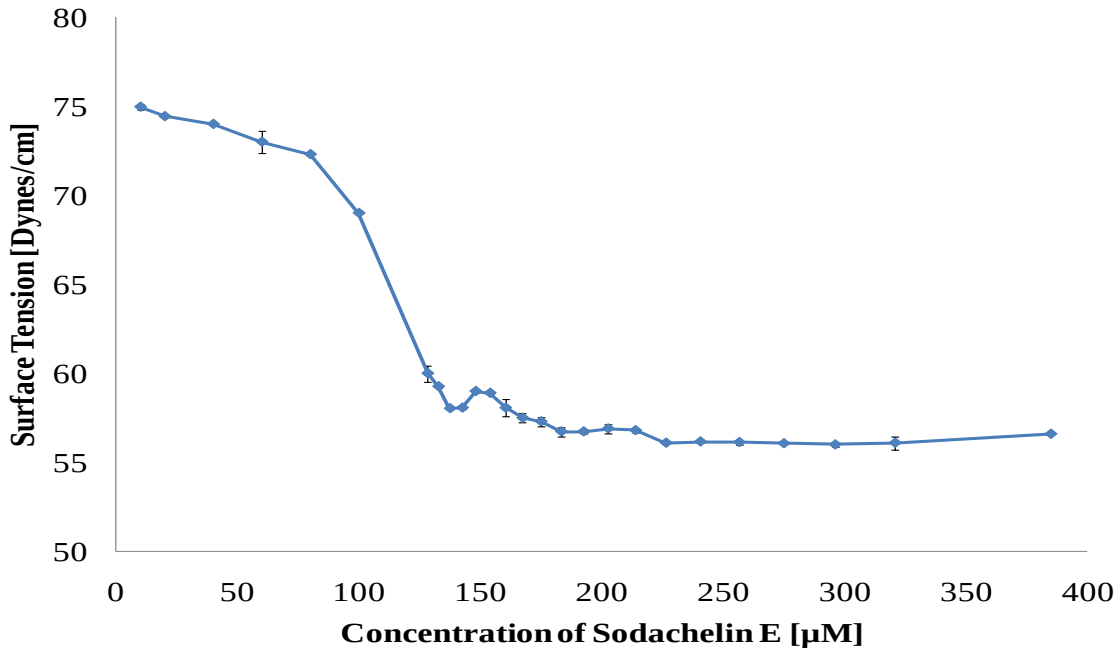

Figure 3.8. Experimental data from the second CMC experiment for sodachelin E.

CHAPTER 4

DISCUSSION

The results of this study were inconclusive in terms of defining a CMC for sodachelin E. The inability to obtain a true CMC for sodachelin is due to the insufficient purification by HPLC. Surfactant self assembly is affected by a large range of factors, such as the size of the hydrophobic moiety, the nature of the polar head-group, the nature of the counter ion , the salt concentration, pH, temperature, and presence of co-solutes. Perhaps the most influential of all of these is the characteristics of the hydrocarbon tail. Amphiphilic siderophores such the marinobactins and the sodachelins, contain a peptidic head that coordinates ferric iron as well as a series of fatty acids that are appended at the amine terminus. Like the marinobactins (Martinez et al., 2000), sodachelin E has a relatively low CMC value due to its structural characteristics. Surfactants with similar head-groups but with different tail lengths tend to have very different CMC values. The hydrophobic effect increases with alkyl chain length. The more alkane character an amphiphile possesses, the lower the CMC. As a general rule, the CMC decreases by a factor of 2 for ionic surfactants and by a factor of 3 for non-ionic surfactants following the addition of one methyl group to the surfactant alkyl chain (Holmberg et al., 2002). The extent of the decrease also depends on substituents and functional groups on the alkyl tail, but qualitatively the same effect is observed. An example of a substituent's effect on micelle size is the comparison of *cis* versus *trans* double bonds. An alkyl tail of a surfactant contains a *cis* double bond will have little to no effect on the tail volume, and thus produces little effect on the micelle radius. On the other hand, a *trans* double bond

would most likely increase the alkyl tail volume thereby increasing the micelle radius. Similar to a cell membrane composed of phospholipids, a *trans* double bond located on a alkyl tail of a phospholipid would interfere with packing of the membrane and increases its fluidity (Holmberg et al., 2002).

The head-group dependence is less straightforward as the alkyl chain. Typically, the CMC of non-ionic surfactants is typically lower than that of the ionic ones, particularly at low salt concentrations, which is due to the electrostatic repulsive nature between the charged head-groups and the size of their head-groups. In other words, increasing the head-group size while keeping the chain length the same, for a non-ionic surfactants, will result in a larger CMC value (Israelachvili et al., 1977). Another consequence of increasing head-group size is the increase in head-group repulsion and packing in a surfactant molecule. A larger head-group tends to increase the curvature of the aggregate, and hence results in smaller and more spherical micelles (Nagarajan and Ruckenstein, 1991). Owen et al.(2005) showed that marinobactins micelle radius is a function of hydrocarbon tail volume and the area of surfactant head-group.

$$R = 3v/a$$

Where R is the micelle radius, v is the hydrocarbon tail volume and a is the area of the head-group. Upon the addition of Fe(III) to the marinobactins, a decrease in micelle radius and CMC is observed due to ionic solute effects, this will be explained later in the chapter. Owen et al. (2005) observed an increase in head-group area upon the coordination of Fe(III) and a decrease in micelle diameter as well as CMC.

Co-solutes, such as oil, salt, and alcohols, can also have a dramatic effect on CMC values. Upon the addition of salt to ionic surfactants, the electrostatic repulsion between the head-groups is shielded. As a consequence, the repulsive interaction opposing micellization becomes relatively less important and the attractive driving force for micellization therefore dominates, resulting in smaller CMC values (Nagarajan and Ruckenstein, 1991). For non-ionic surfactants, increasing ionic strength has little effect on micellization due to the lack of ionic head-groups until high salt concentrations (0.1 – 1 M), are reached where lypotropic salt effects are observed. Lower CMC values would be observed, compared to CMC values obtained in a non-ionic solution of water, for the sodachelins present in Soap Lake due to the high salt content of the microbial environment.

Like the addition of salt, the addition of hydrocarbons to the surfactant-water solution can have a dramatic affect on the CMC. At times, hydrophobic solutes such as oils can decrease the CMC of a surfactant. From simple space-filling considerations, it is obvious that the solubilization of hydrophobic solutes promotes micellization and decreases the CMC (Lieberman et al., 1996).

As mentioned previously, CMC values are not only affected by addition of solutes to an amphiphilic solution. Temperature has an interesting affect on the CMC values for both ionic and non-ionic surfactants. For non-ionic surfactants, an increase in temperature results in a decrease in repulsion amongst the polar head-groups. Micellization is thus favored at higher temperatures, making CMC values lower. The

temperature dependence for ionic surfactants is the opposite due to entropic reasons (Lieberman et al., 1996).

The sodachelins produced by SL28 are exposed to high mineral content due to the chemical nature of Soap Lake (Richards, 2007). The minerals, specifically transition metal ions, could prompt the sodachelins to produce multi-lamellar vesicles in the presence of excess metal ions. Owen et al. (2005) has shown that the marinobactins aggregate into multi-lamellar vesicles in the presence of excess Fe(III). As mentioned previously, the marinobactins are a single-chained amphiphile with a polar head-group. Such compounds typically form spherical micelles primarily because spherical micelles have lower aggregation numbers thus micellization is thermodynamically favored over vesicles (Israelachvili et al., 1977). Surfactants, such as phospholipids, that contain more than one alkyl tail have a more rod-like geometry which favors vesicle formation. Amphiphilic siderophores typically have a cone-shaped geometry and are predisposed to forming micelles, however, in the presence of excess iron, amphiphilic siderophores will bind together, by the bridging of head-groups, and have a more rod-like structure, similar to that of a phospholipid. The rod-like structures, as mentioned previously, will favor a vesicular arrangement over a micellular one due to the change in geometry (Israelachvili et al., 1977; Sommerdijk et al., 1999; Luo et al., 2002a).

In addition to allowing head-groups to pack closer together upon the coordination of Fe(III), the coordination of excess Fe(III) by anionic terminal carboxylate group on the marinobactins decreases the overall negative charge of the bilayer. The decrease in charge of unilamellar vesicle bilayers could induce the formation of multilamellar

vesicles by decreasing the repulsive force between anionic bilayers (Sommerdijk et al., 1999). Fe(III) is not the only metal to promote vesicle formation amongst amphiphilic siderophores. Owen et al. (2008) have had positive vesicle formation with the addition of other metals such as Cd(II), Zn(II) and La(II). On the other hand, K(I) and Na(I) ions cannot promote vesicle formation with single tailed amphiphiles (Luo et al., 2002a), *d*-orbitals on heavier metals appear to have a significant influence.

Impurities and irregularities in the experimental process of determining the CMC will have a dramatic impact on surface tension values obtained from an instrument like the Tensiomat. The protocol developed for this study was consistent as long as clean glassware was used, a constant temperature, and with consistent surface equilibration times. The most important aspect for consistency is the rate at which tension is applied to the torsion arm. The semi-auto mode ensures a smooth consistent rate and very accurate experimental data.

In a non-ionic solution of neutral pH, our first attempt at determining the CMC for sodachelin E was not successful due to an inability to achieve micellization. We predicted that the CMC would fall within 25µM to 150 µM, based on published values of amphiphilic siderophores of similar structure (Martinez et al., 2000). Based on a plot of surface tension versus concentration, even the stock solution with a concentration of 300 µM appears not to have been sufficiently concentrated to promote micellization of sodachelin E. Also, based on our HPLC/UV chromatogram of the stock solution, Figure 3.7, it appears that the siderophore isolated by HPLC is not purely sodachelin E. A trace amount of sodachelin F is present, as well as a significant impurity of unknown origin.

This impurity appears in the chromatogram at a much later retention time than that of sodachelin E and this impurity is most likely creating some error in the stock solution concentration and may also be affecting micelle formation.

The second attempt at determining the CMC value for sodachelin E used a stock solution of 385 µM. Unlike the first experiment, a CMC value of approximately 140 µM for sodachelin E was observed. Such a high CMC value is unexpected in light of the structural characteristics of this amphiphile with its longer chain length. Martinez et al. (2000) have reported CMC values between 25 µM and 50 µM for amphiphilic siderophores with similar head-group structures and alkane character. When the stock solution was analyzed by HPLC, the same impurities were detected in the second experiment as in the first. These impurities perhaps created an inaccuracy in determining the exact concentration of the amphiphilic stock solutions and may have impacted micelle formation. The reason for the absence of a micelle formation from the first experiment is not quite clear. Most likely it is due to the impurities present in the first lyophilized samples that would lead to inaccuracies in weighing. As mentioned earlier, the large broad peak located later in the chromatogram after sodachelin F must have some significant hydrophobic properties. Hydrophobic solutes can affect the CMC values of a surfactant. A second purification step on the HPLC is necessary to generate a pure solution of sodachelin E.

CHAPTER 5

CONCLUSIONS AND FUTURE WORK

Conclusions

To the best of our knowledge, this work documents the first effort to characterize the CMC of sodachelin E. The sodachelins bear a strong structural resemblance to other amphiphilic siderophores, like the marinobactins and the aquachelins, which would suggest similar aggregation characteristics. The *Halomonas sp.* SL28 reached maximum siderophore production after 45 hours of incubation. The isolation of siderophores from the supernatant is best accomplished best using an XAD resin. The XAD resin has a strong affinity for these amphiphiles and is more efficient at crude separation of large amounts of cell-spent supernatant than the smaller C2 cartridges. After concentrating the crude material using XAD separation, purification by HPLC is reasonable, but these results show that collected fractions should be purified a second time to minimize contamination. Elimination of contaminants will permit a more accurate measurement of the CMC value for sodachelin E. The protocol that was developed in this paper to measure CMC values is accurate and consistent based on the CMC value obtained from the SDS experiment, but elimination of contaminants is essential.

Future Work

Immediate future work would be a second purification experiment of sodachelin E by HPLC to obtain a product of higher purity. This would permit a measurement of the

actual CMC value by surface tension measurements. Additional experiments would include the isolation and purification of SL28's five remaining siderophores and their measurement of their respective CMC values.

Micellization for anionic amphiphiles can be highly dependent on ionic strength and pH of the solution. A matrix of experiments could be conducted, based on previously published methods (Martinez et al., 2000; Rice et al., 2004), to determine the effect of high/low pH and high/low salinity on the formation of micelles by the sodachelins. Micelle formation can be ascertained by the Tensiomat and vesicle formation and size can be determined using dynamic light scattering (DLS), cryogenic transmission electron microscopy (cryo-TEM), and UV-vis spectroscopy methods. Long-term vesicle stability could also be examined under a variety of conditions, such as prolonged high or low pH conditions and exposure to prolonged elevated temperature.

Micelle and vesicle formation by amphiphilic siderophores of similar structures have been observed following the addition of excess Fe(III) and various other metals (Owen et al., 2005; Owen et al., 2008). Structural characteristics of micelles and vesicles formed by the sodachelins could be described by using small angle neutron scattering (SANS) and DLS. DLS analyses are limited to particles of ~7 nm, depending on the instrument, and would be best for characterizing vesicles. SANS analyses can be used to determine micelle and vesicle size, shape and composition.

Siderophore-Fe(III) binding and metal-bridging vesicle induction for the sodachelins has not been characterized. Owen et al. (2008) have used X-ray absorption spectroscopy (XAS) to study local geometric and electronic structures of marinobactins

bound to metals. XAS data can provide information on structural orientation and bonding characteristics of organic molecules bound to metals. In addition, Fe(III) is paramagnetic, so electron paramagnetic resonance (EPR) can be used to determine the distances between ferrated siderophores based on dipolar line broadening effects.

REFERENCES

Abergel, R. J., Wilson, M. K., Arceneaux, J. E., Hoette, T. M., Strong, R. K., Byers, R., et al. (2006). Anthrax Pathogen Evades Mammalian Immune System Through Stealth Siderophore Production. *Proceeding of the National Academy of Sciences of the United States of America , 103* (49), 18499-18503.

Albrecht-Gary, A. M., & Crumbliss, A. L. (1998). Coordination Chemistry of Siderphores: Thermodynamics and Kinetics of Iron Chelation and Release. *Metal Ions in Biological Systems , 35*, 239-327.

Anderson, G. C. (1958). Seasonal Characteristics of Two Saline Lakes in Washington. *Limnology and Oceanography , 3* (1), 51-68.

Andrews, S. C., Robinson, A. K., & Rodriguez-Quinones, F. (2003). Bacterial Iron Homeostasis. *FEMS Microbiology Reviews , 27* (2-3), 215-237.

Archibald, F. (1983). Lactobacillus Plantarum, an Organism not Requiring Iron. *FEMS Microbiological Letters , 19*, 29-32.

Arnow, L. E. (1937). Colorimetric Determination of the Components of 3,4-Dihydroxyphenylalanine Tyrosine Mixtures. *Journal of Biological Chemistry , 118* (2), 531-537.

Barbeau, K., Rue, E. L., Bruland, K. W., & Butler, A. (2001). Photochemical Cycling of Iron in the Surface Ocean Mediated by Microbial Iron(III)-Binding Ligands. *Nature , 413* (6854), 409-413.

Beck, R., Abe, Y., Terabayashi, T., & Hoffmann, H. (2002). A Novel L3-Phase from a Ca-salt of an Anionic Surfactant and a Cosurfactant. *The Journal of Physical Chemistry B , 106* (13), 3335-3338.

Boos, W. (1998). Binding Protein-Dependent ABC Transport System for Glycerol 3-phosphate of Escherichia Coli. *Methods in Enzymology , 292*, 40-51.

Boukhalfa, H., & Crumbliss, A. L. (2002). Chemical Aspects of Siderophore Iron Transport. *BioMetals , 15* (4), 325-339.

Boukhalfa, H., Brickman, T. J., Armstrong, S. K., & Crumbliss, A. L. (2000). Kinetics and Mechanism of Iron(III) Dissociation from the Dihydroxamate Siderophores Alcaligin and Rhodotorulic Acid. *Inorganic Chemistry , 39* (25), 5591-5602.

Budzikiewicz, H. (2005). Bacterial Citrate Siderophores. *Mini-Review in Organic Chemistry , 2* (2), 119-124.

Budzikiewicz, H. (2003). Heteroaromatic Monothioccarboxylic Acids from Pseudomonas spp. *Biodegradation , 14* (2), 65-72.

Butler, A. (2005). Marine Siderophores and Microbial Iron Mobilization. *BioMetals , 18* (4), 369-374.

Byers, B. R., & Arceneaux, J. E. (1998). Microbial Iron Transport: Iron Acquisition by Pathogenic Microorganisms. In A. Sigel, & H. Sigel (Eds.), *Metal Ions in Biological Systems* (pp. 37-66). New York: Marcel Decker.

Csaky, T. Z. (1948). On the Estimation of Bound Hydroxylamine in Biological Materials. *Acta Chemica Scandinavica , 2*, 450-454.

De Voss, J. J., Rutter, K., Schroeder, B. G., & Barry, C. E. (1999). Iron(III) Acquisition and Metabolism by Mycobacteria. *Journal of Bacteriology , 181* (15), 4443-4451.

Desnoyers, J. E., & Gerald, P. (1997). Thermodynamic Properties of Surfactant Solutions. In K. S. Birdi (Ed.), *Handbook of Surface and Colloid Chemistry* (pp. 119-156). New York: CRC Press.

Dimitriu, P. A., Shukla, S. K., Conradt, J., Marquez, M. C., Ventosa, A., Maglia, A., et al. (2005). Nitrincola Lacisaponensis Gen. Nov., sp Nov., A novel Alkaliphilic Bacterium Isolated from an Alkaline, Saline Lake. *International Journal of Systematic and Evolutionary Microbiology , 55*, 2273-2278.

Domingue, P. A., Mottle, B., Morck, D. W., Brown, M. R., & Costerton, J. W. (1990). Simplified Rapid Method for the Removal of Iron and Other Cations from Complex Media. *Journal of Microbiological Methods , 12* (1), 13-22.

Dreshel, H., & Winkelmann, G. (1997). Iron Chelation and Siderophores. In G. Winkelmann, & C. J. Carrano (Eds.), *Transition Metals in Microbial Metabolism* (pp. 1-49). Amsterdam: Hardwood Academic.

Granger, J., & Price, N. M. (1999). The importance of siderophores in iron nutrition of heterotrophic marine bacteria. *Limnology and Oceanography , 44* (3), 541-555.

Guerinot, M. L. (1994). Microbial Iron Transport. *Annual Review of Microbiology , 48*, 743-772.

Herrington, K. L., Kaler, E. W., Miller, D. D., Zasadzinski, J. A., & Chiruvolu, S. (1993). Phase-Behavior of Aqueous Mixtures of Dodecyltrimethylammonium Bromide (DTAB) and Sodium Dodecyl-Sulfate (SDS). *Journal of Physical Chemistry , 97* (51), 13792-13802.

Hiemenz, P. C. (1986). *Principles of Colloid and Surface Chemistry* (2 ed.). New York: Marcel Dekker.

Holmberg, K., Jönsson, B., Krongberg, B., & Lindman, B. (2002). *Surfactants and Polymers in Aqueous Solution*. New York:Wiley

Israelachvili, J. N., Marcelja, S., & Horn, R. G. (1980). Physical Principles of Membrane Organization. *13* (2), 121-200.

Israelachvili, J. N., Mitchell, J., & Ninham, B. W. (1977). Theory of Self-Assembly of Lipid Bilayers and Vesicles. *Biochimica et Biophysica , 470*, 185-201.

Jones, B. E., Grant, W. D., Duckworth, A. W., & Owenson, G. G. (1998). Microbial Diversity of Soda Lakes. *Extermophiles , 2*, 191-200.

Koster, W. (1991). Iron(III) Hydroxamate Transport Across the Cytoplasmic Membrane of Escherichia Coli. *Biology of Metals , 4* (1), 23-32.

Lee, K. C., Carlson, P. A., Goldstein, A. S., Yager, P., & Gelb, M. H. (1999). Protection of a Decapeptide from Proteolytic Cleavage by Lipidation and Self-assembly into High-axial-ratio Microstructures: A Kinetic and Structural Study. *Langmuir , 15* (17), 5500-5508.

Lippard, S. J., & Berg, J. M. *Principles of Bioinorganic Chemistry.* Mill Valley: University Science Books.

Litwin, C. M., & Calderwood, S. B. (1993). Role of iron in regulation of virulence genes. *Clinical Microbiology Reviews , 6* (2), 137-149.

Luo, X., Miao, W., Wu, S., & Liang, Y. (2002a). Spontaneous formation of vesicles from octadecylamine in dilute aqueous solution induced by Ag(I) ion. *Langmuir , 18*, 9611-9612.

Luo, X., Wu, S., & Liang, Y. (2002b). Vesicle formation induced by metal ions from micelle-forming sodium hexadecylamino diacetate in dilute aqueous solution. *The Royal Society of Chemistry* , 492-493.

Martinez, J. S., & Butler, A. (2007). Marine amphiphilic siderophores: marinobactin structure, uptake and microbial partitioning. *Journal of Inorganic Biochemistry , 101*, 1692-1698.

Martinez, J. S., Carter-Franklin, J. N., Mann, E. L., Martin, J. D., Haygood, M. G., & Butler, A. (2003). Structure and membrane affinity of a suite of amphiphilic siderophores produced by a marine bacterium. *Proceedings of the National Academy of Sciences of the United States of America , 100* (7), 3754-3759.

Martinez, J. S., Haygood, M. G., & Butler, A. (2001). Identification of a natural desferrioxamine siderophore produced by a marine bacterium. *Limnology and Oceanography , 46*, 420-424.

Martinez, J. S., Zhang, J. P., Holt, P. D., Jung, H. T., Carrano, C. J., Haygood, M. G., et al. (2000). Self-assembling amphiphilic siderophores from marine bacteria. *Science , 287*, 1245-1247.

Mietzner, T. A., Tencza, S. B., Adhikari, P., Vaughan, K. G., & Nowalk, A. K. (1998). Fe(III) periplasm-tocytosol transporters of gram-negative pathogens. *Current Topics in Microbiology and Immunology , 225*, 113-135.

Morel, F. M., & Price, N. M. (2003). The biogeochemical cycles of trace metals in the oceans. *Science , 300* (5621), 944-947.

Nagarajan, R., & Ruckenstein, E. (1991). Theory of surfactant self-assembly: a predictive molecular thermodynamic approach. *Langmuir , 7*, 2934-2969.

Neilands, J. B. (1991). A brief history of iron metabolism. *Biology of Metals , 4* (1), 1-6.

Neilands, J. B. (1993). Siderophores. *Perspectives in Biochemistry and Biophysics , 302* (1), 1-3.

Neilands, J. B. (1995). Siderophores: structure and function of microbial iron transport compounds. *The Journal of Biological Chemistry , 270* (45), 26723-26729.

Owen, T., Pynn, R., Hammouda, B., & Butler, A. (2007). Metal-dependent self-assembly of a microbial surfactant. *Langmuir , 23*, 9393-9400.

Owen, T., Pynn, R., Martinez, J. S., & Butler, A. (2005). Micelle-to-vesicle transition of an iron-chelating microbial surfactant. *Langmuir , 21*, 12109-12114.

Owen, T., Webb, S. M., & Butler, A. (2008). XAS study of a metal-induced phase transition by a microbial surfactant. *Langmuir , 24*, 4999-5002.

Ratledge, C., & Dover, L. G. (2000). Iron metabolism in pathogenic bacteria. *Annual Review of Microbiology , 54*, 881-941.

Raymond, K. N., Dertz, E. A., & Kim, S. S. (2003). An archetype for microbial iron transport. *Proceedings of the National Academy of Sciences of the United States , 100* (7), 3584-3588.

Reid, R. T., Live, D. H., Faulkner, D. J., & Butler, A. (1993). A siderophore from a marine bacterium with an exceptional ferric ion affinity constant. *Nature , 366*, 455-458.

Rice, G., Tang, L., Stedman, K., Roberto, F., Spuhler, J., Gillitzer, E., et al. (2004). The structure of a thermophilic archaeal virus shows a double-stranded DNA viral capsid type that spans all domain of life. *Proceedings of the National Academy of Sciences of the United States of America , 101* (20), 7716-7720.

Richards, A.M. (2007) *Identification and structural characterization of siderophores produced by halophilic and alkaliphilic bacteria*. (Doctoral dissertation, Washington State University, 2007)

Rieger, M. M. (1996). Surfactants. In H. A. Lieberman, M. M. Rieger, & G. S. Banker (Eds.), *Pharmaceutical Dosage Forms: Disperse Systems* (Second ed., Vol. 1, pp. 211-286). New York: Marcel Dekker.

Schwyn, B., & Neilands, J. B. (1987). Universal chemical assay for the detection and determination of siderophores. *Analytical Biochemistry , 60,* 47-56.

Scott, B. M., Paszczynski, A. J., Korus, R., & Crawford, R. L. (2003). The Determination of the Stability Constant for the Iron(II) Complex of the Biochelator Pyridine-2,6-bis(monothiocarboxylic acid). *Biodegradation , 14* (2), 73-82.

Sommerdijk, N. A., Booy, K. J., Pistorius, A. M., Feiters, M. C., Nolte, R. J., & Zwanenburg, B. (1999). Copper(II) complexes of a dicephalic imidazole surfactant. Tunable organization of metalloaggregates. *Langmuir , 15,* 7008-7013.

Sorokin, D. Y., Foti, M., Pinkhart, H. C., & Muyzer, G. (2007). Sulfur-oxidizing bacteria in Soap Lake (Washington State), a meromictic, haloalkaline lake with an unprecedented high sulfide content. *Applied and Environment Microbiology , 73* (2), 451-455.

Spasojevic, I., & Crumbliss, A. L. (1999). pH Induced Active ("Uphill") Liquid Membrane Transport of Ferrioxamine B by the Ionizable Ionophore Lasalocid. *Inorganic Chemistry , 38* (13), 3248-3250.

Szymczyk, K., & Janczuk, B. (2009). Thermodynamics of micellization of aqueous solutions of binary mixtures of two anionic surfactants. *Langmuir , 25* (8), 4377-4383.

Touati, D. (2000). Iron and oxidative stress in bacteria. *Archives of Biochemistry and Biophysics , 373* (1), 1-6.

Ventosa, A., Marquez, M. C., Garabito, M. J., & Arahal, D. R. (1998). Moderately halophilic Gram-positive bacterial diversity in hypersaline environments. *Extremophiles , 2* (3), 297-304.

Winkelmann, G. (Ed.). (1991). *Handbook of Microbial Iron Chelates.* Boca Raton: CRC Press.

Winkelmann, G. (2002). Microbial siderophore - mediated transport. *Biochemical Society Transactions , 30* (4), 691-696.

Xu, G., Martinez, J. S., Groves, J. T., & Butler, A. (2002). Membrane affinity of the amphiphilic marinobactin siderophores. *Journal of the American Chemical Society , 124* (45), 13408-13415.

APPENDICES

APPENDIX A

RAW DATA FOR GROWTH AND PRODUCTION OF SIDEROPHORES

Table A1: Raw data for siderophore production at pH 9 using the optical density at 600 nm to track cell growth and the optical density at 630 nm for the CAS assay to determine siderophore production.

Date	Time	Hours	pH 9 OD 600	pH 9 OD 630
3/25/2009	13:00	0	0.011	0.944
			0.010	0.953
			0.011	0.958
	17:00	4	0.017	0.948
			0.018	0.96
			0.017	0.97
	21:00	8	0.118	0.943
			0.118	0.967
			0.118	0.95
3/26/2009	1:00	12	0.196	0.943
			0.196	0.944
			0.194	0.966
	5:00	16	0.291	0.933
			0.276	0.916
			0.27	0.922
	9:00	20	0.4	0.898
			0.381	0.929
			0.373	0.929
	13:00	24	0.477	0.663
			0.46	0.695
			0.445	0.763
	17:00	28	0.554	0.301
			0.536	0.368
			0.532	0.474
	21:00	32	0.58	0.488
			0.568	0.529
			0.554	0.579
3/27/2009	1:00	36	0.56	0.752
			0.562	0.729
			0.536	0.752
	9:00	44	0.571	0.715
			0.562	0.725
			0.55	0.714
	21:00	56	0.524	0.825
			529	0.841
			0.534	0.837
3/28/2009	9:00	68	0.516	0.825
			0.523	0.841
			0.524	0.891

APPENDIX B

RAW DATA AND GRAPH FOR CAS CALIBRATION CURVE

Table B.1. Raw data for CAS calibration curve used to calculate siderophore concentration based on DFB equivalence. Absorbance measured at 630 nm.

DFB Concentration [µM]	Optical Density at 620 nm		
	1	2	3
0	0.922	0.911	0.911
1	0.875	0.873	0.881
2	0.836	0.851	0.834
5	0.729	0.730	0.736
8	0.596	0.596	0.582
10	0.507	0.496	0.502
12	0.408	0.393	0.390
15	0.296	0.260	0.264
18	0.172	0.163	0.171
20	0.130	0.116	0.125

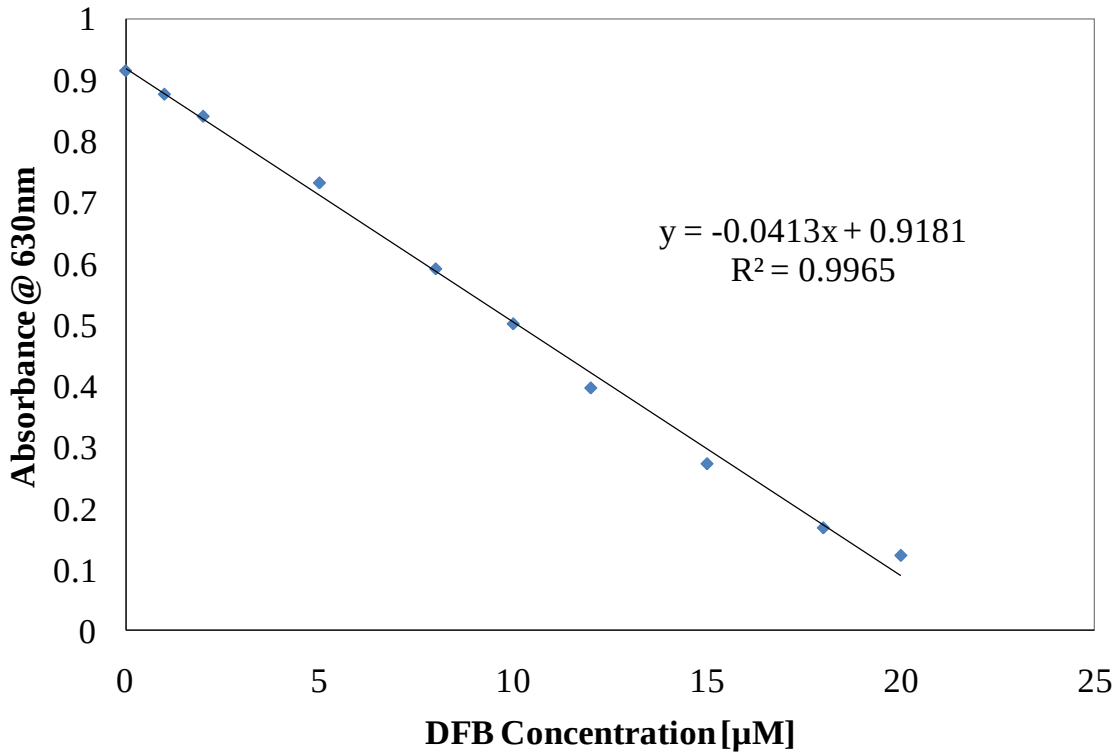

Figure B.1. CAS calibration curve and linear equation used to calculate siderophore concentration. Linear equation derived by least squares method.

APPENDIX C

RAW DATA FROM TIMED TENSIOMAT EXPERIMENT

Table C.1. Raw data from timed tensiomat experiment with SDS as the control.

Mode	Concentration [mM]	Temperature [Celsius]	Time [s]	Surface Tension [Dynes/cm]		
				1	2	3
Manual	5	22.1	30	49.1	48.0	47.5
			60	47.0	47.0	47.0
			90	47.0	47.0	46.9
			120	47.2	47.1	47.2
Semi-Auto	5	22.1	30	48.0	47.9	48.0
			60	48.0	48.0	48.0
			90	48.1	48.0	48.0
			120	47.9	48.1	48.0
Semi-Auto	10	23.2	30	41.2	41.1	41.1
			60	41.2	41.1	41.1
			90	41.5	41.4	41.3
			120	41.1	41.2	41.2
			180	41.2	41.2	41.1

APPENDIX D

RAW DATA FROM CMC EXPERIMENT WITH SDS

Table D.1. Surface tension data from SDS experiment.

Mode	Time [s]	Temperature [Celsius]	Concentration [mM]	Surface Tension [Dynes/cm]		
				1	2	3
Semi-Auto	30	23.1	0.1	73.2	74.5	74.5
			0.2	72.9	73	73
			0.4	68.9	66.3	67
			0.8	64.5	64.9	64
			1	61	59.5	61
			2	52.8	54.5	55.1
			4	49.9	50	50
			8	41.1	41.2	41
			10	42	42.1	42.2
			20	42	42	42
			40	41.5	41	42
			50	41	41	41.5

APPENDIX E

RAW DATA FROM CMC EXPERIMENTS WITH SODACHELIN E

Table E.1. Surface tension data from first CMC experiment with sodachelin E.

Mode	Time [s]	Temperature [Celsius]	Concentration [µM]	Surface Tension [Dynes/cm]		
				1	2	3
Semi-Auto	30	22.9	2	75.0	75.0	75.0
			4	75.0	75.0	75.0
			8	74.0	74.5	74.5
			10	75.0	74.5	74.5
			20	75.0	74.0	74.0
			40	74.0	73.0	73.0
			60	72.0	71.0	71.0
			80	67.0	67.0	67.0
			100	65.0	64.0	65.0
			120	64.0	63.0	63.0
			140	61.0	61.0	60.5
			160	59.0	58.9	58.0
			180	58.0	58.0	57.9
			200	56.0	56.0	55.0
			220	55.0	55.0	54.0
			240	52.0	52.0	52.0
			260	52.9	52.0	51.9
			280	51.9	51.0	50.0
			300	50.2	49.5	49.0

Table E.2. Surface tension data from second CMC experiment with sodachelin E.

Mode	Time [s]	Temperature [Celsius]	Concentration [µM]	Surface Tension [Dynes/cm]		
				1	2	3
Semi-Auto	30	23.1	10	57.0	56.3	56.5
			20	56.0	56.2	56.1
			40	56.0	56.0	56.0
			60	56.0	56.2	56.0
			80	56.1	56.2	56.1
			100	56.2	56.1	56.2
			128	56.2	56.1	56.0
			133	57.0	56.5	56.9
			138	56.9	56.8	57.0
			143	56.5	56.7	57.0
			148	57.0	56.5	56.7
			154	57.5	57.4	57.0
			160	57.0	58.0	57.5
			167	58.1	58.0	58.1
			175	58.9	58.8	59.0
			183	59.0	58.9	59.1
			193	58.0	58.1	58.1
			203	58.0	58.1	58.0
			214	59.0	59.8	59.0
			226	60.0	60.0	60.0
			241	69.0	69.0	69.0
			257	73.0	72.0	71.9
			275	73.0	72.9	73.1
			296	74.0	74.0	74.0
			321	74.5	74.5	74.3
			385	75.0	74.9	75.0